SUPPLEMENTAL INFORMATION

SUPPLEMENTAL FIGURE S1

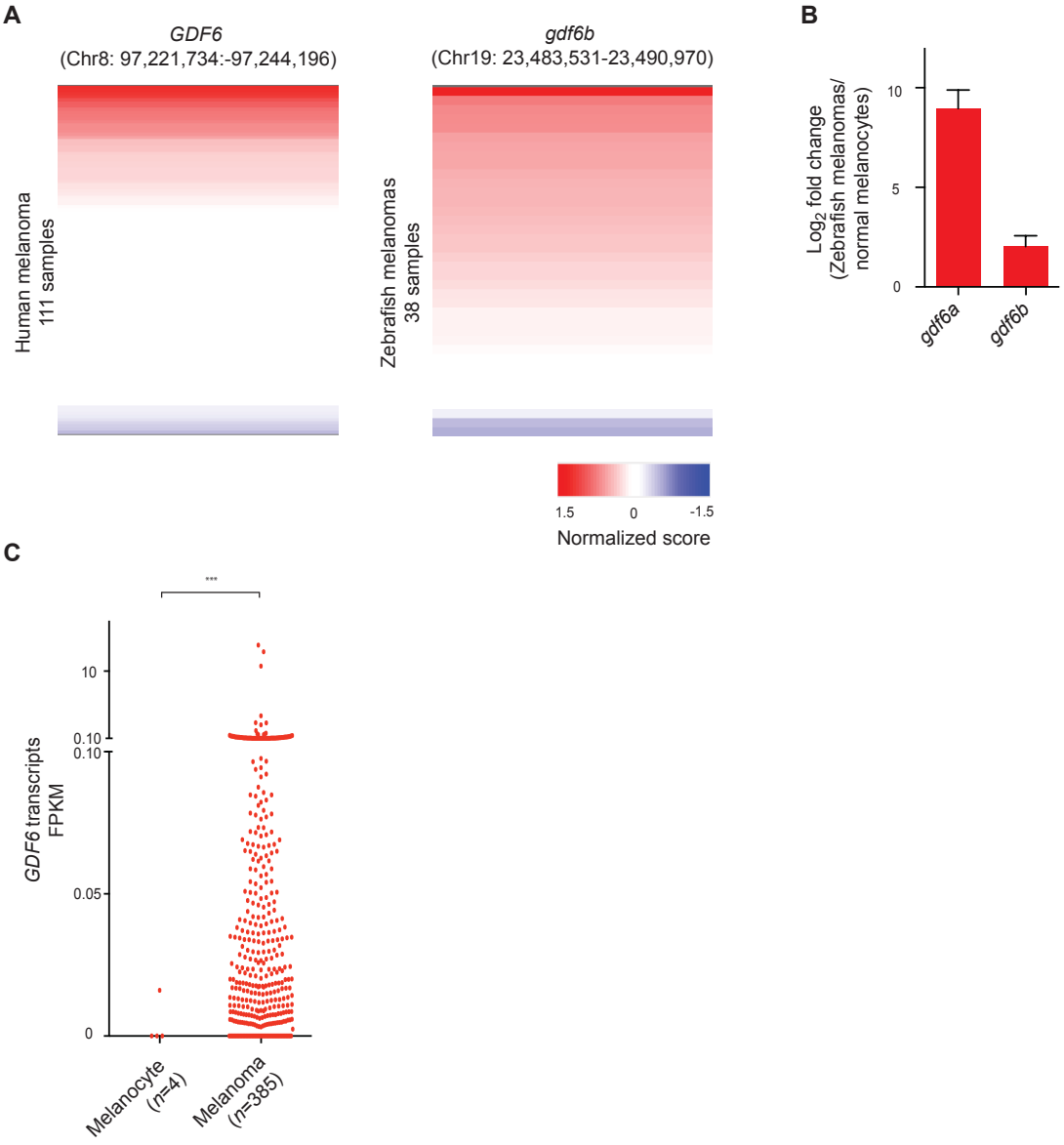

Supplemental Figure S1: *GDF6* orthologs are amplified and upregulated in human and zebrafish melanomas

(**A**) Heat map showing the human *GDF6* locus across 111 human melanomas (left) and the zebrafish *gdf6b* locus across 38 zebrafish melanomas (right). Red indicates amplification, blue indicates deletion. (**B**) Log2-transformed fold change of *gdf6a* and *gdf6b* expression in zebrafish melanomas as compared to melanocytes as determined by qRT-PCR. (**C**) *GDF6* transcript FPKM values from normal human melanocytes and melanomas. ****P*<0.001 by two-tailed Welch's *t*-test.

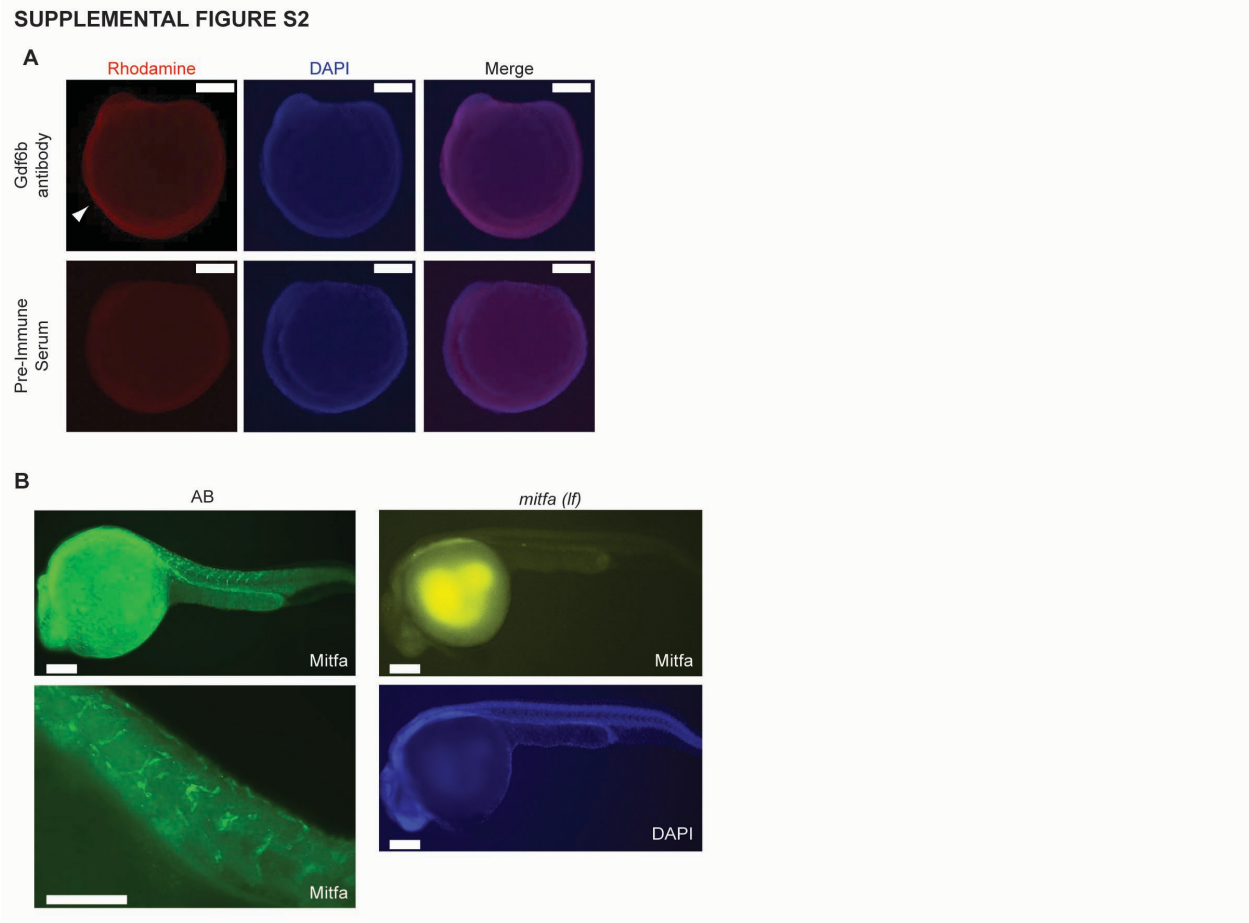

Supplemental Figure S2: Specificity of zebrafish Gdf6b and Mitfa antibodies
(**A**) Immunostaining with Gdf6b antibody (top) and pre-immune serum (bottom) in 4-somite stage AB embryos. Expression of Gdf6b is seen in the neural plate (arrow head) as described previously (1). Scale bars, 100 μM. (**B**) Left, immunostaining with Mitfa antibody in wild-type AB zebrafish embryos. Right, immunostaining with Mitfa antibody in *mitfa(lf)* zebrafish embryos. Mitfa (top), DAPI (bottom). Scale bars, 100 μM.

SUPPLEMENTAL FIGURE S3

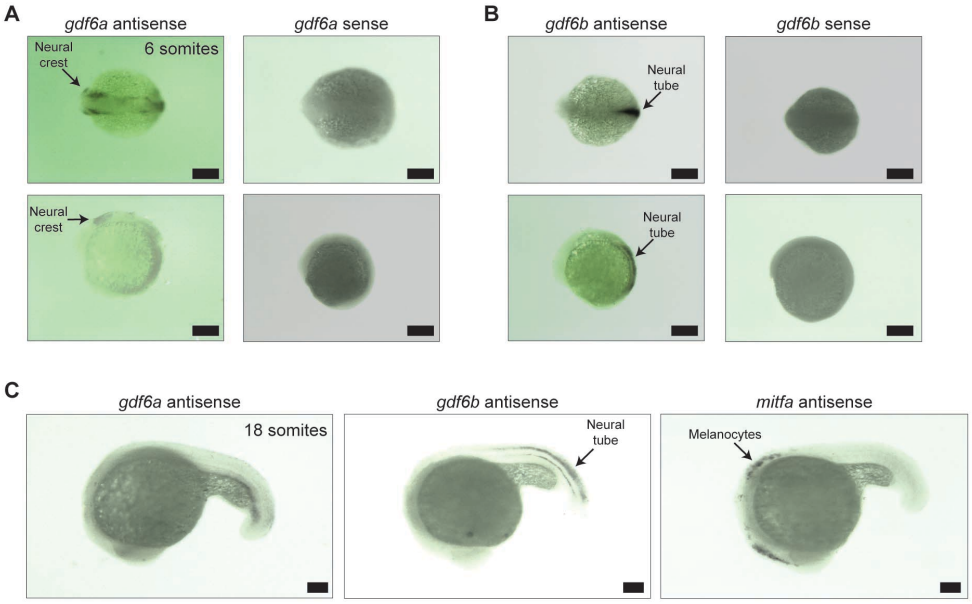

Supplemental Figure S3: Expression of zebrafish *GDF6* orthologs during embryonic development

(**A**) *In situ* hybridization with *gdf6a* antisense probe showing expression of *gdf6a* in the neural crest at the 6-somite stage. A *gdf6a* sense probe was used as a negative control. Top, dorsal view. Bottom, lateral view. Scale bar, 100 μM (**B)** *In situ* hybridization with *gdf6b* antisense probe showing expression of *gdf6b* in the neural tube at the 6-somite stage. A *gdf6b* sense probe was used as a negative control. Top, dorsal view. Bottom, lateral view. Scale bar, 100 μM (**C**) *In situ* hybridization with *gdf6a* and *gdf6b* probes showing their lack of expression at the 18-somite stage. *In situ* hybridization of *mitfa* shows melanocyte specification at this stage. No *gdf6a* or *gdf6b* staining was found in developing melanocytes. Scale bar, 100 μM.

SUPPLEMENTAL FIGURE S4

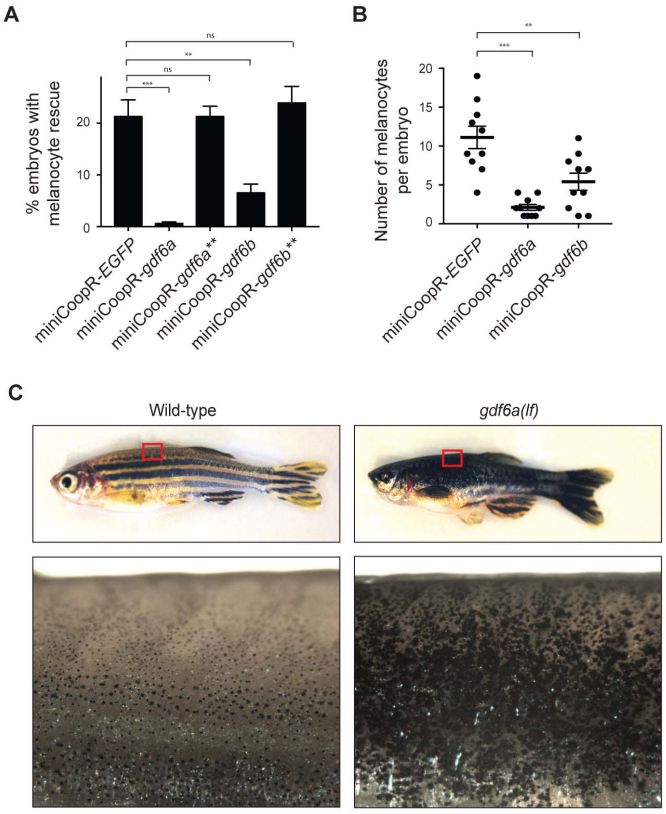

Supplemental Figure S4: Effects of zebrafish *GDF6* orthologs on melanocyte number

(A) Quantification of the fraction of zebrafish embryos with melanocyte rescue following injection of indicated miniCoopR constructs in *Tg(mitfa:BRAFV600E);p53(lf);mitfa(lf)* zebrafish. *gdf6a*** and *gdf6b*** are forms of *gdf6a* and *gdf6b* with premature stop codons, respectively. Error bars indicate s.e.m.: *n*=3 independent experiments. **(B)** Quantification of the number of melanocytes per rescued embryo. Error bars indicate s.e.m.: *n*=10 embryos. (**C**) Representative images of *Tg(mitfa:BRAFV600E);p53(lf);gdf6a(lf)/+* and *Tg(mitfa:BRAFV600E);p53(lf);gdf6a(lf)* zebrafish. Boxed region from the top panel is shown in the bottom panel. ***P*< 0.01, ****P*< 0.001, ns, not significant, by one-way ANOVA with Dunnett test.

SUPPLEMENTAL FIGURE S5

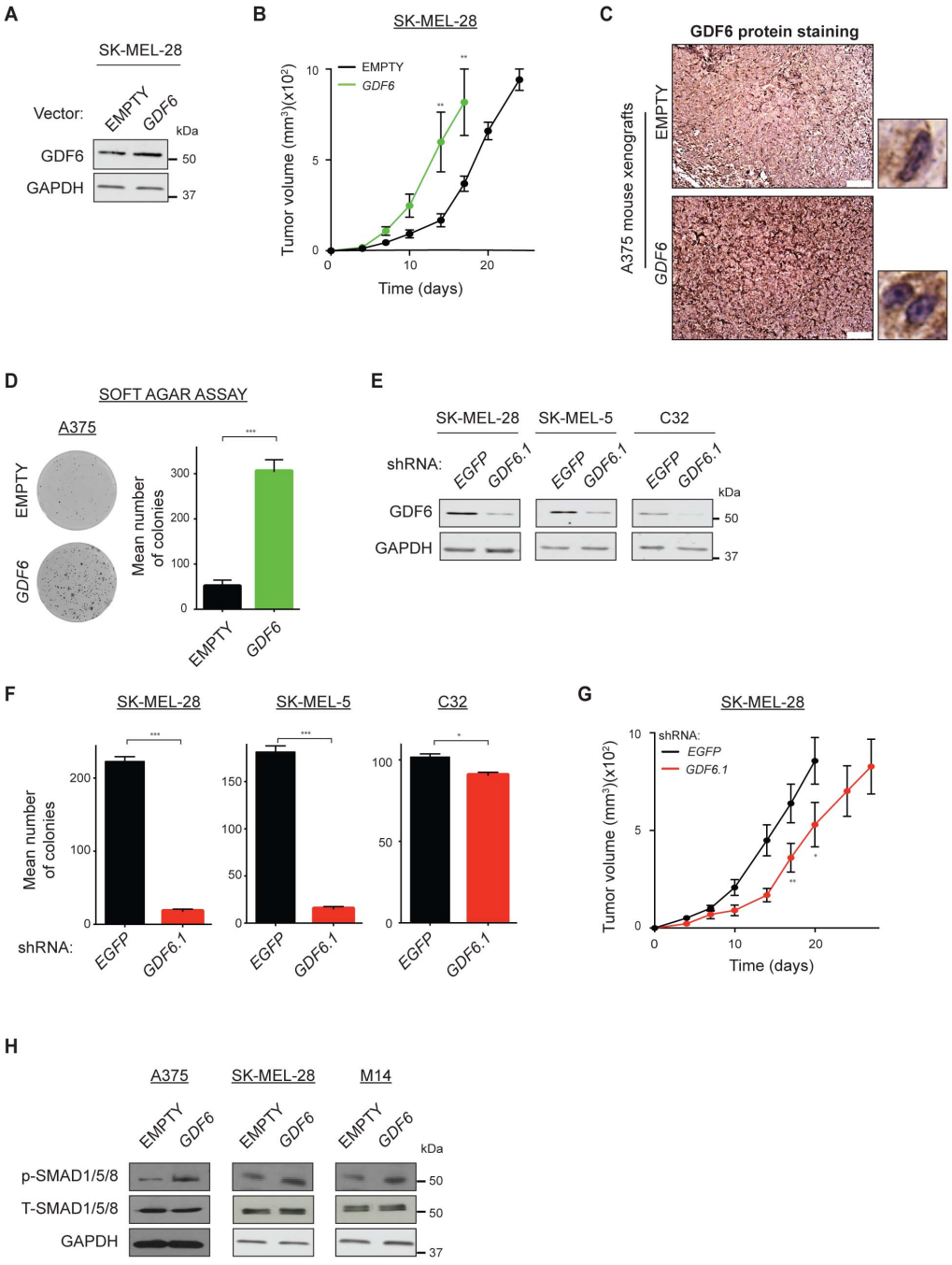

Supplemental Figure S5: *GDF6* modulation alters the tumorigenicity of human melanoma cells

(**A**) Immunoblots of GDF6 and GAPDH from SK-MEL-28 melanoma cells overexpressing *GDF6*. (**B**) Tumor formation in mice injected with SK-MEL-28 cells ($1x10^6$ cells injected per mouse) overexpressing *GDF6* or empty vector control. Error bars indicate s.e.m.; *n*=3. (**C**) GDF6 staining of mouse xenografts with A375 melanoma cells overexpressing *GDF6* as compared to empty vector control. Scale bars, 50 µm. Single cells are shown on the right. (**D**) Soft agar assay with A375 melanoma cells overexpressing *GDF6*. Error bars indicate s.e.m.; *n*=3. (**E**) Immunoblots of GDF6 and GAPDH in melanoma cells

(labeled at top) expressing *shEGFP* or *shGDF6.1*. (**G**) Colony formation assay with melanoma cells (indicated above) expressing *shEGFP* or *shGDF6.1*. Error bars indicate s.e.m.; *n*=3. (**H**) Tumor formation in mice injected with SK-MEL-28 cells ($1x10^7$ cells injected per mouse) expressing an shRNA targeting *EGFP* or the *GDF6*-targeted shRNA, *GDF6.1*. Error bars indicate s.e.m.; *n*=3. (**I**) Immunoblots of phospho-SMAD1/5/8, total SMAD1/5/8 and GAPDH in melanoma cell lines (indicated above) overexpressing *GDF6* or empty vector control. **P*< 0.05, ***P*< 0.01, ****P*< 0.001 by two-tailed Student's *t*-test. For figure panels S5B and S5G, two-tailed Student's *t*-test was performed by comparing tumor volumes of two groups at a given time point.

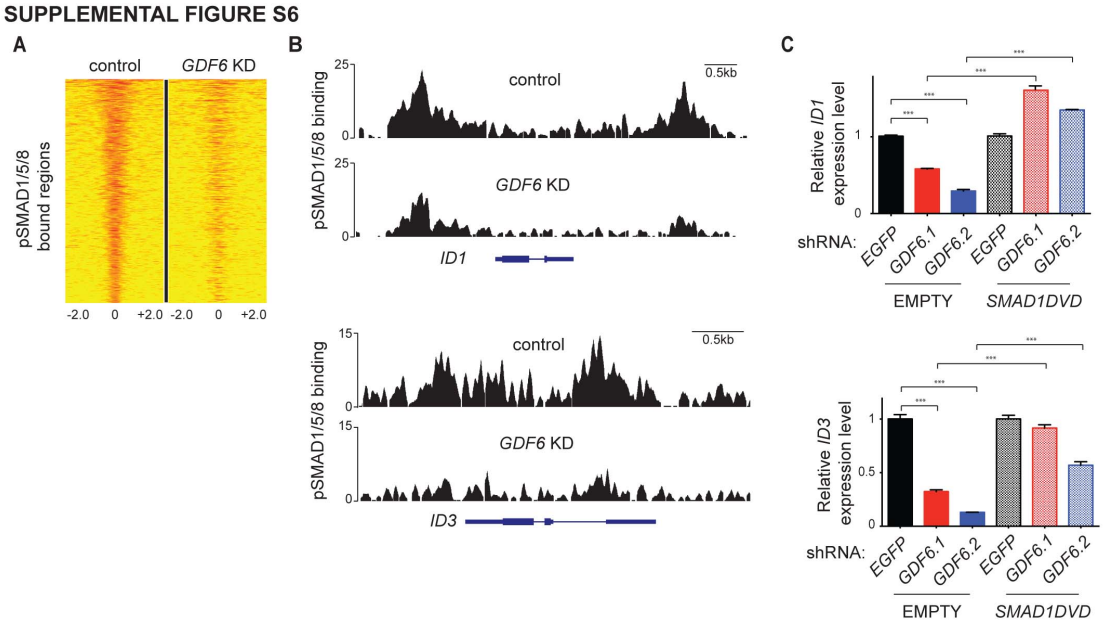

Supplemental Figure S6: *GDF6* knockdown impairs BMP pathway activity
(**A**) Comparison of ChIPseq maps of phospho-SMAD1/5/8 binding in control and *GDF6*-depleted cells. The heat map extends from -2kb to +2kb from the center of each bound region, with each row representing a unique bound region and enrichment denoted in red. The heat map is sorted based on phsopho-SMAD1/5/8 binding in control cells. (**B**) phospho-SMAD1/5/8 binding to the *ID1* locus (top) and *ID3* locus (bottom) in A375 melanoma cells expressing *shEGFP* or *shGDF6.1.* (**C**) qRT-PCR showing expression of *ID1* (top) and *ID3* (bottom) in A375-empty or A375-*SMAD1DVD* cells expressing an shRNA targeting *EGFP* or two independent *GDF6*-targeted shRNAs. Left two brackets, *ID* gene expression is downregulated upon *GDF6* knockdown. Right two brackets, downregulation of *ID* gene expression is reversed in *SMAD1DVD*-expressing cells upon *GDF6* knockdown. Error bars indicate s.e.m.; *n*=3. ***P< 0.001 by one-way ANOVA with Bonferroni test.

SUPPLEMENTAL FIGURE S7

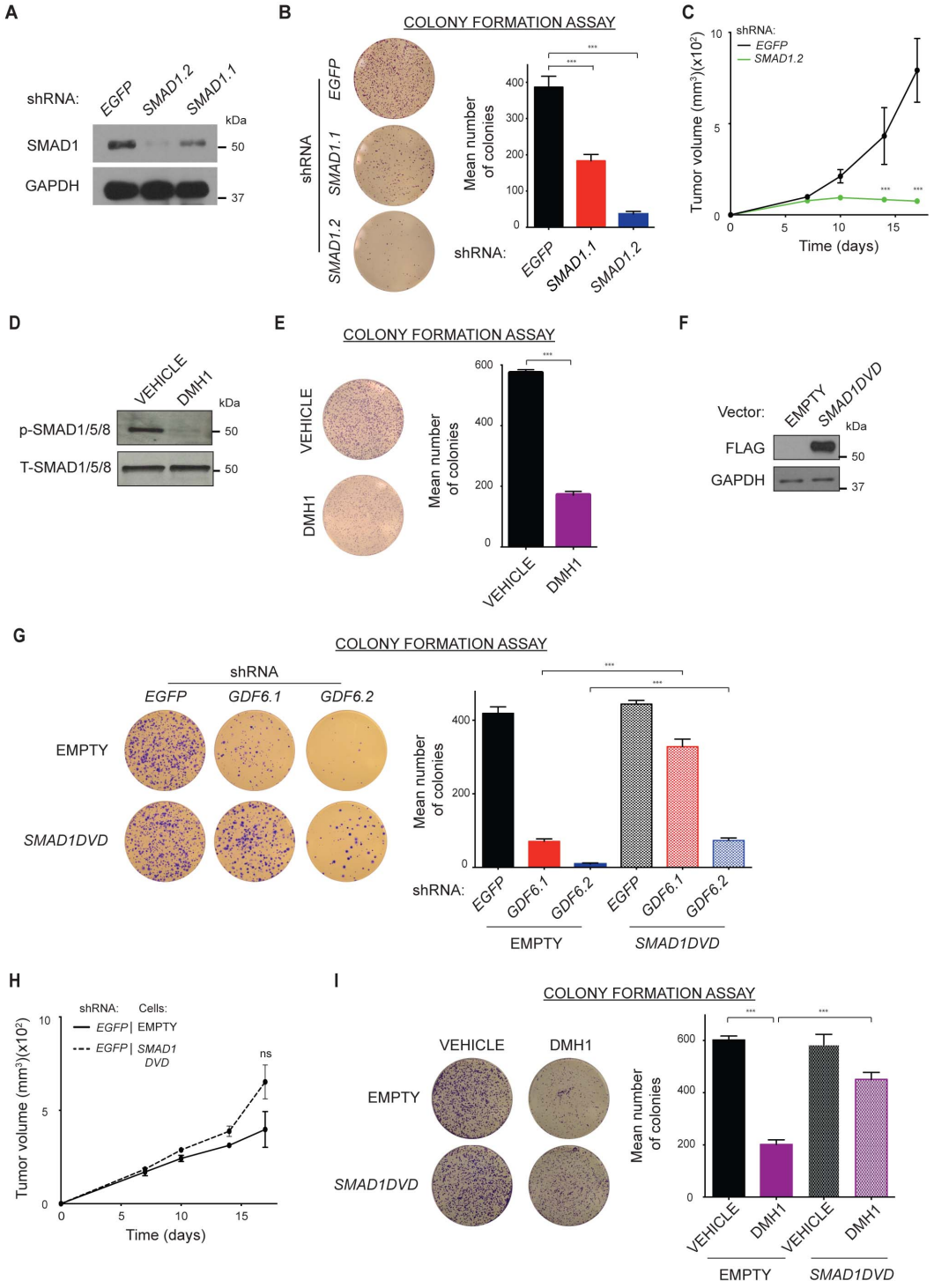

Supplemental Figure S7: *GDF6* acts through SMAD1 to promote melanoma progression

(**A**) Immunoblots showing expression of SMAD1 and GAPDH in A375 melanoma cells expressing *shEGFP*, *shSMAD1.1* or *shSMAD1.2*. (**B**) Colony formation assay with A375

cells expressing *shEGFP*, *shSMAD1.1* or *shSMAD1.2*. Error bars indicate s.e.m.; *n*=3. (**C**) Tumor formation in mice injected with A375 cells expressing *shEGFP* or *shSMAD1.2*. Error bars indicate s.e.m.; *n*=3. (**D**) Immunoblots showing expression of phospho-SMAD1/5/8 and total SMAD1/5/8 in A375 melanoma cells after treatment with 0.1% DMSO (vehicle) or 10μM DMH1 in 0.1% DMSO. (**E**) Colony formation assay with A375 cells treated with 0.1% DMSO (vehicle) or 10μM DMH1 in 0.1% DMSO. Error bars indicate s.e.m.; *n*=3. (**F**) Immunoblots showing expression of Flag-tagged SMAD1DVD and GAPDH in control and A375-*SMAD1DVD* cells. (**G**) Colony formation assay with A375-EMPTY or A375-*SMAD1DVD* cells expressing *shEGFP*, *shGDF6.1* or *shGDF6.2*. Error bars indicate s.e.m.; *n*=3. (**H**) Tumor formation in mice injected with A375-empty or A375-*SMAD1DVD* cells expressing an *EGFP*-targeted shRNA**.** Each mouse was injected with $1x10^7$ cells. Error bars indicate s.e.m.; *n*=3. (**I**) Colony formation assay with A375-empty or A375-*SMAD1DVD* cells treated with 0.1% DMSO (vehicle) or 10μM DMH1 in 0.1% DMSO. Error bars indicate s.e.m.; *n*=3. ****P*< 0.001, ns, not significant, by one-way ANOVA with Dunnett test (B), two-tailed Student's *t*-test (C, E, H), or one-way ANOVA with Bonferroni test (G, I).

SUPPLEMENTAL FIGURE S8

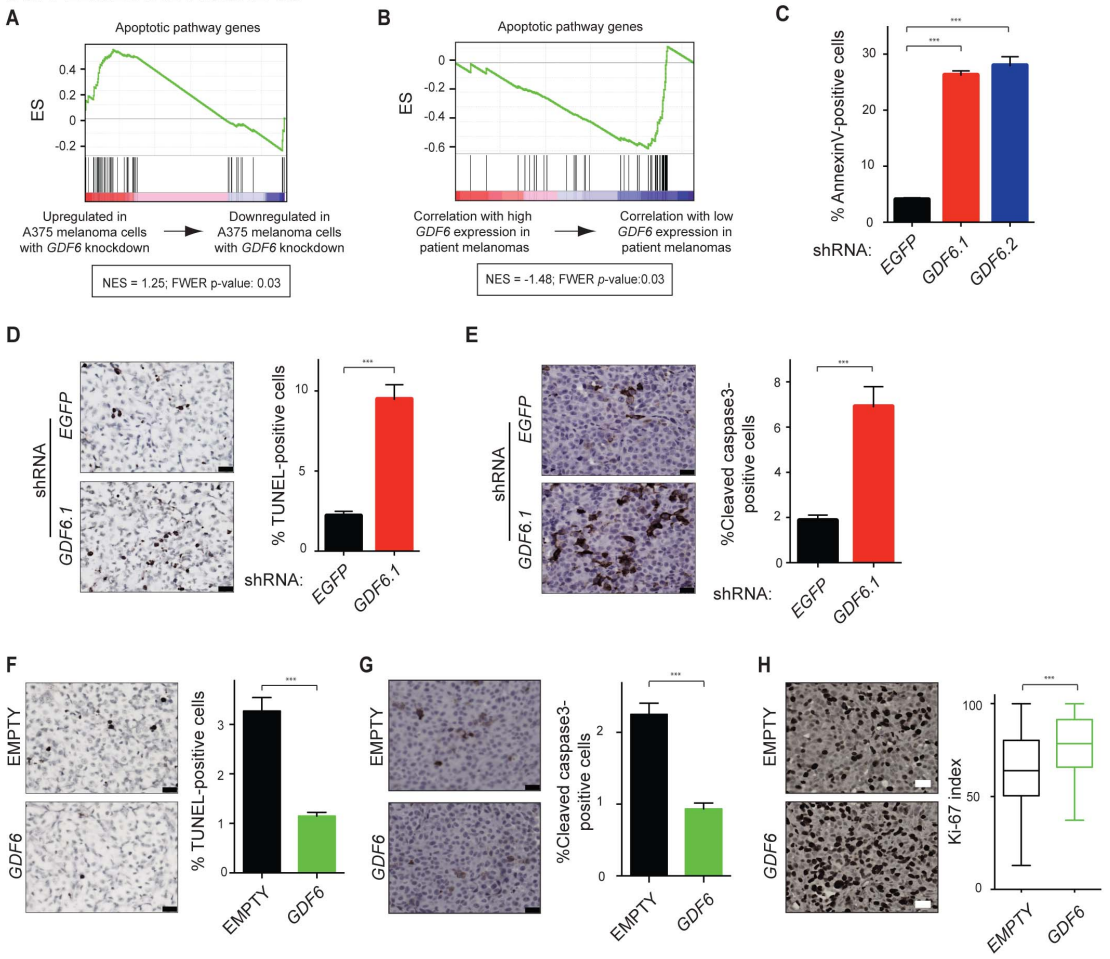

Supplemental Figure S8: *GDF6* knockdown causes melanoma cell death
(**A**) GSEA shows that expression of an apoptotic gene set (MSigDB- M10169) is positively enriched in *GDF6*-knockdown A375 cells (**B**) GSEA shows that expression of an apoptotic gene set (MSigDB- M10169) is negatively enriched in patient-derived melanomas (TCGA) expressing high levels of *GDF6*. (**C**) Flow cytometry analysis of annexinV-positivity of A375 cells upon *GDF6* knockdown. Error bars indicate s.e.m.; *n*=3. (**D**) TUNEL staining of mouse xenografts of A375 cells upon *GDF6* knockdown. Scale bar, 25μm. Error bars indicate s.e.m.; *n*=100 fields. (**E**) Cleaved Caspase-3-staining of mouse xenografts of A375 cells upon *GDF6* knockdown Scale bar, 25μm. Error bars indicate s.e.m.; *n*=100 fields. (**F**) TUNEL staining of mouse xenografts of A375 cells upon *GDF6* overexpression. Scale bar, 25μm. Error bars indicate s.e.m.; *n*=100 fields. (**G**) Cleaved Caspase-3-staining of mouse xenografts of A375 cells overexpressing *GDF6* or empty vector control. Scale bar, 25μm. Error bars indicate s.e.m.; *n*=100 fields. (**H**) Ki-67 staining of mouse xenografts of A375 cells overexpressing *GDF6* or empty vector control. Scale bar, 25μm. Right, quantification of Ki67-positive cells (Ki-67 index); Error bars indicate s.e.m.; *n*=100 fields. ***$P < 0.001$ by one-way ANOVA with Dunnett test (C) or two-tailed Student's *t*-test (D, E, F, G, H).

SUPPLEMENTAL FIGURE S9

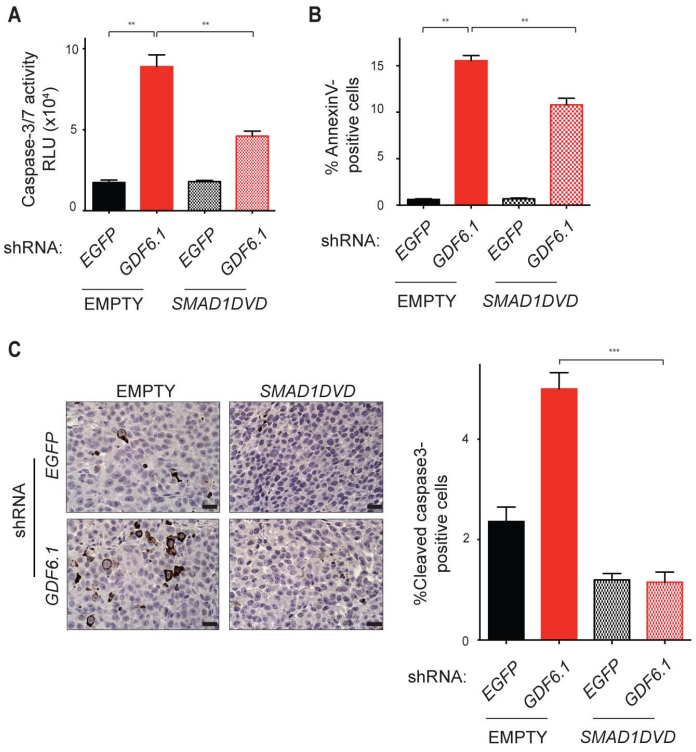

Supplemental Figure S9: *GDF6* knockdown-induced cell death is rescued by *SMAD1DVD*

(**A**) Caspase-3/7 activity measured as relative luciferase units (RLU) in A375-empty or A375-*SMAD1DVD* cells expressing an shRNA targeting *EGFP* or the *GDF6*-targeted shRNA, *GDF6.1*. Error bars indicate s.e.m.; *n*=3. (**B**) Flow cytometry analysis of annexinV-positivity of A375-empty or A375-*SMAD1DVD* cells expressing an shRNA targeting *EGFP* or the *GDF6*-targeted shRNA, *GDF6.1*. Error bars indicate s.e.m.; *n*=3. (**C**) Cleaved Caspase-3 staining of mouse xenografts of A375-empty or A375-*SMAD1DVD* cells expressing an shRNA targeting *EGFP* or the *GDF6*-targeted shRNA *GDF6.1*. Scale bar, 25μm. Error bars indicate s.e.m.; *n*=100 fields. ***P*< 0.01, ****P*< 0.001 by one-way ANOVA with Bonferroni test.

SUPPLEMENTAL FIGURE S10

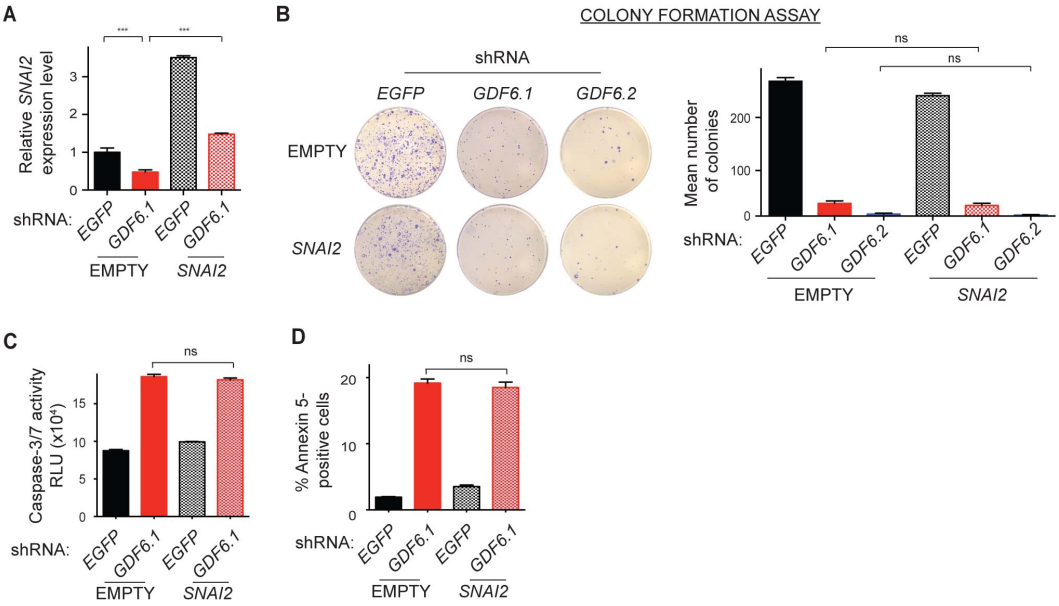

Supplemental Figure S10: *SNAI2* overexpression does not rescue growth defects and cell death caused by *GDF6* knockdown

(**A**) qRT-PCR showing expression of *SNAI2* in A375-empty or A375-*SNAI2* cells expressing *shEGFP* or *shGDF6.1*. Error bars indicate s.e.m.; n=3. Left bracket, *SNAI2* expression is downregulated upon *GDF6* knockdown. Right bracket, *SNAI2* overexpression in *GDF6* knockdown cells. (**B**) Colony formation assay of A375-empty (top) or A375-*SNAI2* (bottom) cells expressing an shRNA targeting *EGFP* or two independent *GDF6*-targeted shRNAs. Error bars indicate s.e.m.; *n*=3. (**C**) Caspase-3/7 activity measured as relative luciferase units (RLU) in A375-empty or A375-*SNAI2* cells expressing *shEGFP* or *shGDF6.1*. Error bars indicate s.e.m.; *n*=3. (**D**) Flow cytometry analysis of annexinV-positivity of A375-empty or A375-*SNAI2* cells expressing *shEGFP* or *shGDF6.1*. Error bars indicate s.e.m.; *n*=3. ***P< 0.001, ns, not significant, one-way ANOVA with Bonferroni test.

SUPPLEMENTAL FIGURE S11

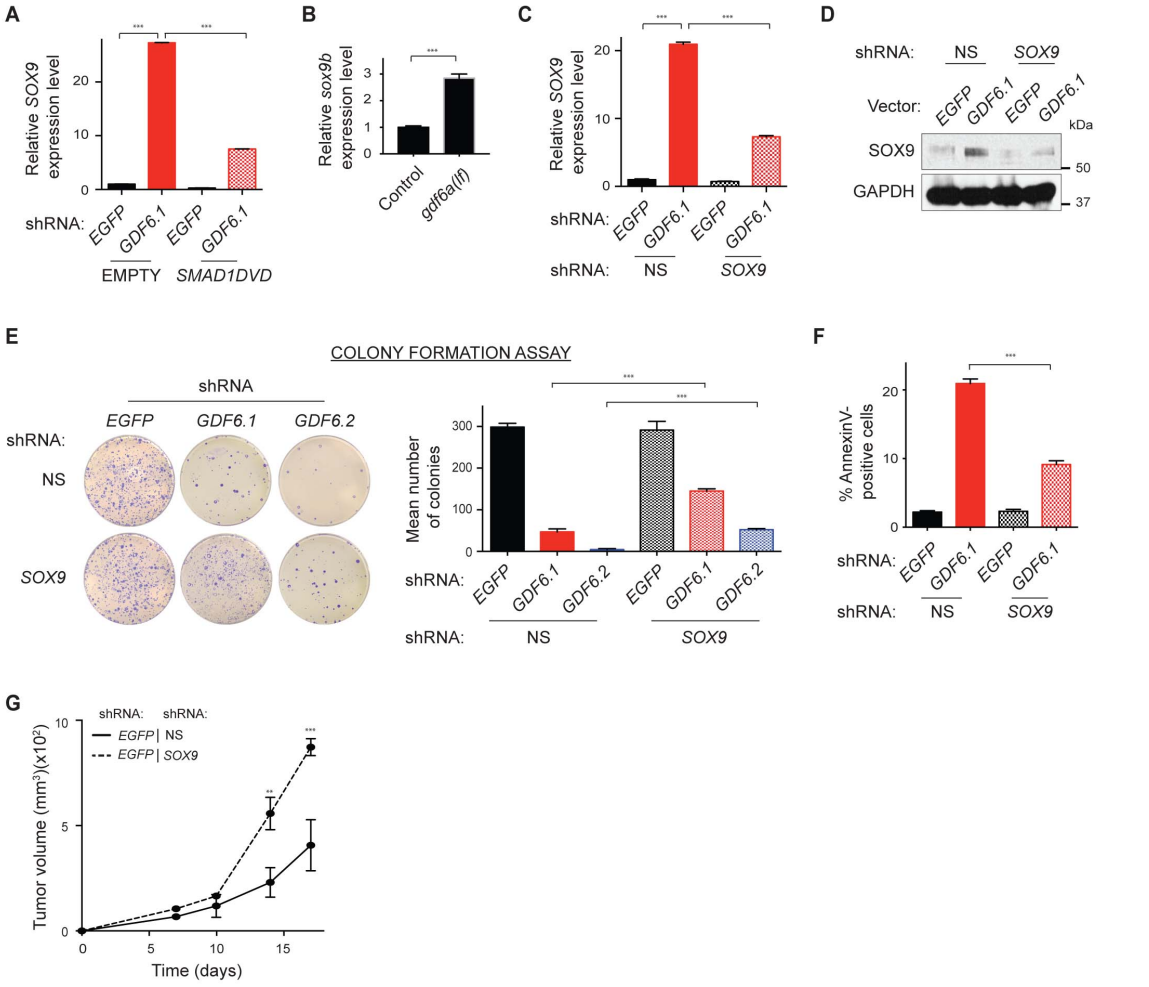

Supplemental Figure S11: *SOX9* knockdown rescues the growth defects and cell death caused by *GDF6* knockdown

(**A**) qRT-PCR of *SOX9* in A375-empty or A375-*SMAD1DVD* cells with *GDF6* knockdown. Error bars indicate s.e.m.; *n*=3. Left bracket, *SOX9* expression is upregulated upon *GDF6* knockdown. Right bracket, *SOX9* expression is less upregulated in *SMAD1DVD*-expressing cells upon *GDF6* knockdown. (**B**) qRT-PCR showing expression of *sox9b* in control and *gdf6a(lf)* zebrafish melanomas. Error bars indicate s.e.m.; *n*=3. (**C**) qRT-PCR showing expression of *SOX9* in A375-non-silencing or A375-*shSOX9* cells with *GDF6* knockdown. Error bars indicate s.e.m.; *n*=3. Left bracket, *SOX9* expression is upregulated upon *GDF6* knockdown. Right bracket, knockdown of *SOX9* expression in *GDF6* knockdown cells. (**D**) Immunoblots showing expression of SOX9 and GAPDH in A375-non-silencing or A375-*shSOX9* cells expressing *shEGFP* or *shGDF6.1*. (**E**) Colony formation assay with A375-non-silencing (top) or A375-*shSOX9* (bottom) cells expressing an shRNA targeting *EGFP* or two independent *GDF6*-targeted shRNAs. Error bars indicate s.e.m.; *n*=3. (**F**) Flow cytometry analysis of annexinV-positivity of A375-non-silencing or A375-*shSOX9* cells expressing *shEGFP* or *shGDF6.1*. (**G**) Tumor formation in mice injected with A375-non-silencing or A375-*shSOX9* cells expressing an shRNA targeting *EGFP.* Error bars indicate s.e.m.;

n=3. ***P*< 0.01, ****P*< 0.001. one-way ANOVA with Bonferroni test (A, C, E, F) or two-tailed Student's *t*-test (B, G).

SUPPLEMENTAL FIGURE 12

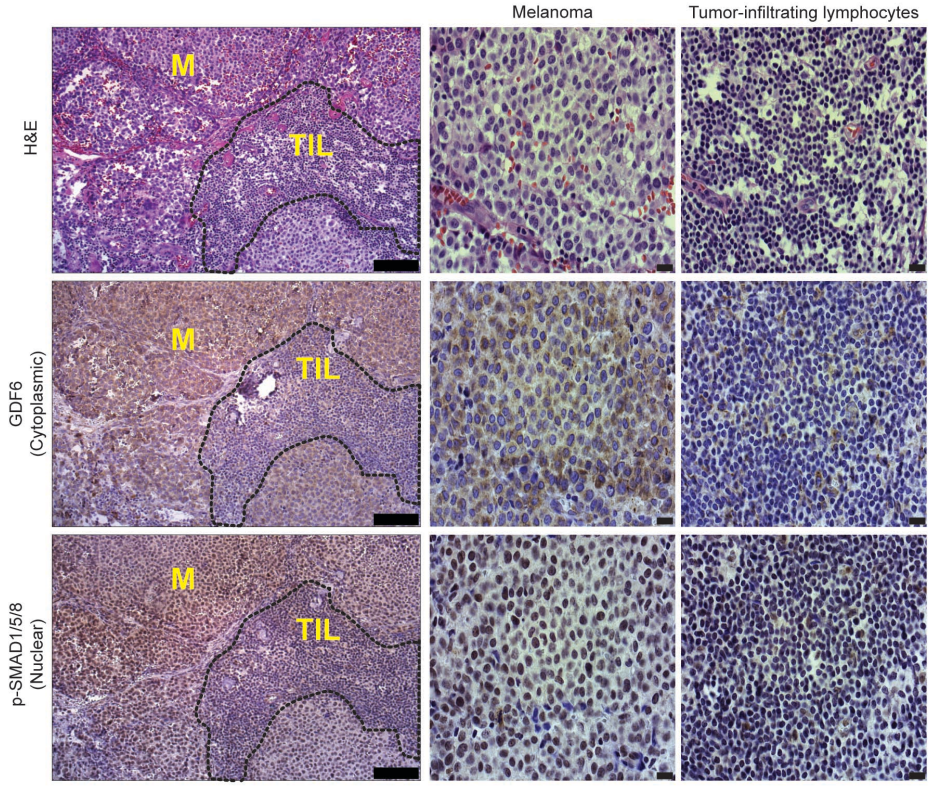

Supplemental Figure S12: GDF6 and phospho-SMAD1/5/8 expression in a patient melanoma section

Section of a metastatic human melanoma (M) with tumor infiltrating lymphoycytes (TIL). Top, hematoxylin and eosin staining. Middle, GDF6 staining. Bottom, phospho-SMAD1/5/8 staining. Left, scale bar, 50 μm. Center and right, melanoma region and TIL region, respectively. Scale bar, 25 μm.

SUPPLEMENTAL FIGURE 13

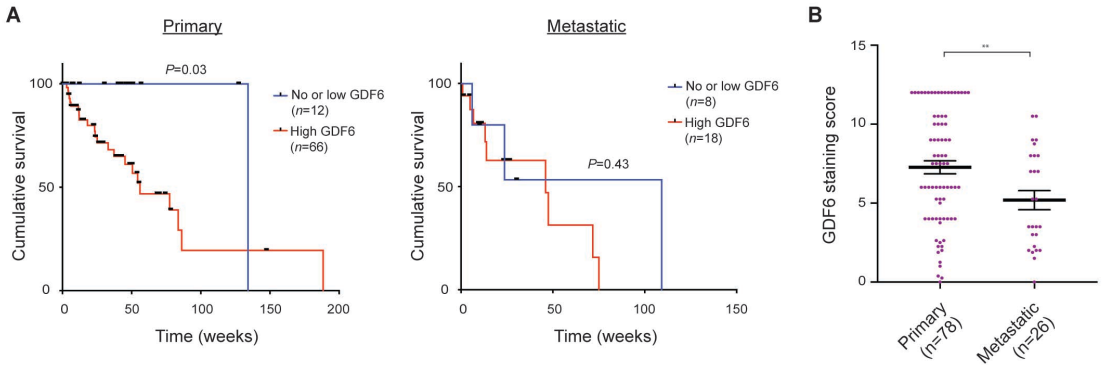

Supplemental Figure S13: Correlation of GDF6 expression with melanoma clinical features

(**A**) Kaplan-Meier analysis showing overall survival of patients (melanoma tissue microarray) with primary melanomas (left) and metastatic melanomas (right) with no or low GDF6 expression (blue line) versus high GDF6 expression (red line). Statistical analysis was performed with a Mantel-Cox log rank test. (**B**) GDF6 expression score in primary and metastatic melanomas from the melanoma tissue microarray. ***P*< 0.01 by two-tailed Welch's *t*-test.

Supplemental Methods

Growth curve, clonogenic and soft agar assays

For growth curves 50,000 live cells were seeded per well in a 6-well tissue culture plate on day 0. The numbers of live cells were calculated every day using an automated cell counter (Nexcelom Bioscience Cellometer Auto T4) following standard procedures. All assays were performed with technical replicates. For clonogenic assays, 3,000 live cells were seeded in a 10 cm tissue culture plate. After 3 weeks, colonies were fixed and stained using bromophenol blue in acetone. ImageJ was used to quantify the number of colonies. In assays with DMH1 treatment, control or DMH1-containing media was replaced every other day. For soft agar assays a 0.5% bottom layer (1:1 with 1% agar and 2XDMEM with 20% FBS) and a 0.3% top layer (1:1 with 0.6% agar and 2XDMEM with 20% FBS) were used. 3,000 live cells per well of a 6-well tissue culture plate were added in the top layer. Media was added initially then replaced every 3 days. After 3 weeks, colonies were stained with nitroblue tetrazolium chloride overnight at 37°C. Once stained, individual wells were photographed, and ImageJ was used to count the number of colonies. All these assays were done in triplicate, and experiments were repeated at least twice.

Cell death assays

A375 melanoma cells after stable knockdown and/or overexpression were stained for Annexin V and 7-AAD (BD Pharmingen PR Annexin V Apoptosis Detection kit) as per manufacturer's instructions, followed by flow cytometry using a FACSCalibur instrument (BD Biosciences). Caspase3/7 activity was measured using the Caspase-Glo 3/7 assay (Promega) as per manufacturer's instructions.

Animal experiments

All animal protocols were approved by the UMMS Institution Animal Care and Use Committee (A-2016, A-2171). Mice were randomly allocated to individual experimental groups. No blinding was done as animal groups were identified by tagging and cage labeling. Animals were excluded, according to pre-established criteria, if the tumor volume reached >1,000 mm^3; if tumor size or location affected the mobility or general health of animal, the animal was euthanized and excluded from the experiment or the complete experiment was terminated.

Antibody production

Antibodies recognizing Gdf6b were generated by injecting a glutathione S-transferase-tagged *gdf6b*, GST-*gdf6b*, into two guinea pigs. Antibodies were validated by comparing reactivity of pre- and post-immune sera to bacterially-expressed GST-*gdf6b*. Results from one of the antibodies are shown.

Immunofluorescence

For adults, dorsal scales bearing normal melanocytes or melanomas were plucked from anesthetized zebrafish. After fixation, scales were bleached of melanin pigment to visualize fluorescence after staining. Scales were incubated with primary antibody (Gdf6b (1:250), Mitfa (1:250)) overnight. Subsequently the scales were washed, incubated in appropriate secondary antibodies (Jackson Labs), incubated with DAPI, mounted on slides with Vectashield (Vectorlabs), and visualized using confocal fluorescence microscopy.

Immunoblotting

Protein extracts were separated on 12% SDS-PAGE gels. Blots were probed with primary antibodies (GDF6 (Sigma PRS4691; 1:1000), phospho-SMAD1/5/8 (Cell Signaling 13820; 1:1000), SMAD1 (Cell Signaling 9743; 1:500), Total SMAD1/5/8 (Santa Cruz sc-6031-R; 1:1000), FLAG (Sigma F3165, 1:2000), SOX9 (Cell Signaling 82630S; 1:1000), GAPDH (Abcam 8245; 1:2000)) overnight at 4°C, washed five times in TBS plus 0.1% Tween (TBST) and then incubated with the appropriate HRP-conjugated secondary antibody (Jackson Labs) for 1 hour at room temperature. Membranes were washed five times in TBST and visualized on autoradiography film after incubating with ECL reagent (Supersignal West Pico or Supersignal West Femto; Thermo Scientific).

Immunohistochemistry (IHC) and TUNEL staining

From mouse xenografts, formalin-fixed, paraffin-embedded tissues were processed to obtain 5μm sections. Sections were stained with H&E, cleaved Caspase-3 (Cell signaling 9664; 1:100), Ki-67 (Dako M7240; 1:100) and evaluated. TUNEL staining was performed on sections using the In Situ Cell Death Detection kit (Roche) as per manufacturer's protocol. The numbers of TUNEL-positive or cleaved Caspase-3-positive or Ki67-positive cells were counted manually and the total number of cells in each field was calculated using ImageJ software.

Individual patient melanoma and tissue microarray cores consisted of 5 μm sections of formalin-fixed, paraffin-embedded tissues. Slides were first deparaffinized with two changes of xylene, and rehydrated with changes of decreasing concentrations of alcohols, then rinsed in distilled water. Antigen retrieval was carried out with 0.01M citrate buffer at pH 6.0, or 0.001M EDTA at pH 8.0. Slides were heated in a 770W microwave oven for 14 minutes, cooled to room temperature, and rinsed in distilled water. The sections were first blocked for endogenous non-specific protein and peroxidase activity with an application of Dual Endogenous Block (Dako) for 10 minutes,

followed by a buffer wash, followed by staining with antibodies recognizing GDF6 (Sigma PRS4691; 1:1000) and p-SMAD1/5/8 (Cell signaling 9664; 1:100) for 30 minutes. Staining with a second antibody recognizing GDF6 (Sigma HPA045206; 1:100) yielded concordant results. For negative controls, non-immune immunoglobulin G (a cocktail of Mouse Whole IgG and Rabbit Whole IgG (Pierce antibodies 31204 and 31207, respectively; both 1ug/ml)) staining was used. Following a buffer wash, sections were incubated with the EnVision+ Dual Link (Dako) detection reagent for 30 minutes. The sections were washed, and treated with a solution of diaminobenzidine and hydrogen peroxide (Dako) for 10 minutes, to produce the visible brown pigment. After rinsing, a toning solution (DAB Enhancer, Dako) was used for 2 minutes to enrich the final color. The sections were counterstained with hematoxylin, dehydrated, and coverslipped with permanent mounting media. Positive signal was defined as dark brown staining. Scant, or fine granular background staining, or no staining was considered negative. Zebrafish formalin-fixed, 5mM EDTA treated, paraffin-embedded tissues were processed to obtain 5μm transverse sections. Sections were stained for H&E and as mentioned above with p-SMAD1/5/8 (Cell Signaling 9511; 1:150) and coverslipped with permanent mounting media. TUNEL staining was performed on sections with fluorescein-dUTP using In Situ Cell Death Detection kit (Roche) as per manufacturer's protocol. For TUNEL staining, sections were bleached in bleaching solutions (3% hydrogen peroxide 1% Potassium hydroxide) to remove the melanin pigment. The numbers of TUNEL-positive were counted manually and the total number of cells (DAPI positive) in each field was calculated using ImageJ software.

IHC scoring

For both the UMass patient cohort and the tissue microarray, a modified visual semi-quantitative method was used. Sections were scored for immunointensity (0-4) and

immunopositivity (0-3), which were then multiplied. For the UMMS patient cohort, scoring was done by C.J.C. and A.M.V., and the scores were averaged. Scores were verified by A.D. For the tissue microarray cohort, scoring was conducted independently by C.L. and C.B.F.G. and the scores were averaged. Sections with scores less than or equal to four were binned into the low or no staining group and sections with scores greater than four were binned into the high staining group.

in situ hybridization

Embryos were grown at 28.5°C until the desired stage, then dechorionated and fixed in 4% PFA/PBS for 24 hours at 4°C. Following fixation, embryos were dehydrated in methanol and stored at -20°C. For *in situ* hybridization, embryos were rehydrated, permeabilized with proteinase K, and hybridized with digoxigenin-labeled probes in hybridization solution (1:100) overnight at 68°C. Probe mixes were removed, embryos were washed in TBST, and then incubated in blocking solution (0.5% Roche Blocking Reagent in TBST) at room temperature. Subsequently the embryos were incubated in anti-digoxigenin-AP conjugated antibody (Roche) diluted in blocking solution (1:400) overnight at 4°C. Following antibody incubation, the embryos were washed in TBST, and the RNA probes were visualized by incubation in NBT-BCIP solution (NBT-BCIP stock solution from Roche, diluted 1:200 in TBST with 50 mM MgCl2). After staining, embryos were washed in PBS and stored in 4% PFA/PBS at 4°C, then mounted 3% methylcellulose for imaging.

Quantifying melanocyte numbers in embryonic zebrafish

Zebrafish embryos were injected with miniCoopR-*EGFP,* miniCoopR-*gdf6a* or miniCoopR-*gdf6b* at the single-cell stage and then grown at 28.5°C. At 4 days post-fertilization, embryos were visualized under a light microscope to identify ones that had a

chimeric pattern of melanocyte rescue. Additionally, the number of melanocytes per rescued embryo was counted manually.

Chromatin immunoprecipitation (ChIP) sequencing and analysis

ChIP was performed using the Simple ChIP Plus Enzymatic Chromatin IP kit as per manufacturer's instructions (Cell Signaling 9001) with the p-SMAD1/5/8 antibody (Cell Signaling 11971; 1:100). ChIP-DNA from A375 melanoma cells expressing an shRNA targeting *GDF6, GDF6.1* or *EGFP* or a 2% input control was used for library preparation using the TruSeq ChIP Library Prep Kit for ChIP-Seq (Illumina). Fastq files were aligned to the human reference genome (ENSEMBL GRCH37) by Bowtie (version 1.0.0) (2) allowing uniquely mapped reads and removing PCR duplicates. For aggregation plotting, aligned reads were processed in HOMER (3) using annotatePeaks to bin the regions of interest in 20-bp windows resulting in average enrichment with normalized reads for all genes. MACS2 (version 2.1.1.20160226) (4) was used for peak calling. Peaks with a false discovery cutoff of 1% were used. The alignment files were converted to bedGraph files and loaded as custom tracks in the UCSC genome browser to visualize regions of interest. ChIPpeakAnno (version 3.5.12) (5) was used to visualize and compare the overlapping pSMAD1/5/8 peaks for genes bound by pSMAD1/5/8 in wild-type and *GDF6* knockdown A375 cells..

aCGH probe design

We custom designed the G3 array format of 2x400K probes for the Zebrafish ZV9 genome assembly using Agilent's eArray (eArray ID 036041). The array has 398426 unique probes covering 97% of the zebrafish genome (based on Zv9 assembly). The probes are 60 bases long and are spaced across the genome with an average separation of 3550 bases.

aCGH, JISTIC analysis and comparative analysis

aCGH was performed as per Agilent's array-based genomic DNA hybridization protocol. Briefly, genomic DNA was extracted from zebrafish melanomas or a normal region of the same fish using the Qiagen DNeasy Blood and Tissue kit. 5 µg of tumor or matched normal gDNA was fragmented to 200-500bp by sonication (Covaris S220R High Performance Sample Preparation Ultrasonicator System 220x S), labeled in a random-primed reaction using Cy5-dCTP or Cy3-dCTP, respectively, and hybridized in Agilent's hybridization buffer with Cot1 DNA (1mg/ml) at 65°C overnight. Arrays were then washed, and Cy5 and Cy3 signals were measured using an Agilent G2565 Microarray Scanner. Raw data was generated from scanned images with the Agilent Feature Extraction software (v10.7). Raw values were normalized using the Agilent Genomic workbench and copy number alterations were detected. The JISTIC algorithm was used in limited peel-off mode to calculate significantly altered regions, and peak calling was done using a q-value cut-off of 0.25. Gene-based JISTIC G-scores and –log10 transformed q-values are represented using the Circos package (6). For representation of data, the G-score scale for amplifications was 0 (minimum) and 1550 (maximum), and for deletions it was 0 (minimum) and 2150 (maximum). The log10-transformed q-value scale for both amplifications and deletions was 0 (minimum) and 11 (maximum). For human melanomas, copy number data was downloaded from Tumorscape (7, 8), and JISTIC analysis was conducted as described above. Genes from within peaks were pooled to define species-specific sets of recurrently amplified genes. Human orthologs of zebrafish genes were determined using Ensembl (9, 10) and supplemented by performing BLAST (11). Recurrently amplified zebrafish and human genes, as determined by JISTIC, were compared to find the overlapping set of commonly amplified genes.

cDNA amplification and microarray analysis

Total RNA was extracted and prepared from melanoma cells and from normal scale-associated melanocytes of *Tg(mitfa:BRAF(V600E)); p53(lf); alb(lf); Tg(mitfa:EGFP)* zebrafish as described above. Total RNA was amplified using the Nugen Ovation RNA Amplification system V2 as per manufacturer's protocol. For microarrays, amplified cDNA was hybridized to a 385K microarray (NimbleGen 0711105Zv7EXPR) as per manufacturer's protocol. Briefly, amplified cDNA from melanomas and melanocytes were labeled with Cy3 independently, hybridized to the microarray, washed and scanned with a GenePix 4000B Scanner. Images were analyzed and normalized using NimbleScan software, and differentially expressed genes were identified.

Massively parallel RNA sequencing

For zebrafish melanomas and melanocytes, total RNA was isolated as described above and libraries were prepared using the TrueSeq Stranded mRNA Library Prep Kit as per manufacturer's protocol (Illumina). FASTQ files were analyzed using FASTQC v0.10.1(12) to ensure uniform read quality (phred>30). Paired-end reads were aligned to the zebrafish genome using STAR v2.3 (13) (Zv9). The mapped reads were counted using htseq-count (v0.6.0, parameters –t exon) (14) and gene models from the Ensembl transcriptome (9). Analyses of differential gene expression were performed using DESeq2 (15). Orthology to human genes was determined using Ensembl (9, 10) and supplemented by performing BLAST (11). The heatmap of BMP pathway genes (REACTOME_SIGNALING_BY_BMP; MSigDB (Broad Institute)) was created using human orthologs of differentially expressed BMP pathway genes. The fish orthologs of human genes represented are *SMAD5=smad5, SMAD4=si:dkey-239n17.4, ACVR2A=acvr2a, ACVR2B=acvr2b, BMPR1A=bmpr1aa, FSTL1=fstl1b,*

SMAD7=smad7, BMPR2=bmpr2a, SMURF2=smurf2, SMAD6=smad6b, ZFYVE16=zfyve16, SKI=skib, GREM2=grem2, SMURF1=smurf1, UBE2D1=ube2d1, CER1=dand5, NOG=nog, BMP2=bmp2b, BMPR1B=bmpr1bb. For A375 human melanoma cells with *GDF6* and/or *SMAD1DVD* modulation, total RNA was isolated and libraries prepared as described above. Prepared libraries were sequenced using Illumina Hiseq technology (NY Genome Center). FASTQC v0.10.1 (12) was used on the FASTQ sequences for the A375 samples to generate sequence quality reports. Data were analyzed using two different bioinformatics pipelines. In the first pipeline, reads were aligned to the human reference genome (Ensembl GRCh37) using Bowtie2 (v 2-2.1.0) (16) and Tophat2 (v 2.0.9) (17). Samtools (v 0.0.19) (18) and IGV (v 2.3.60) (19) were used for indexing the alignment files and viewing the aligned reads, respectively. Gene expression was quantitated as fragments per kilobase of exon model per million mapped fragments (FPKM) using Cufflinks (v 2.2.0) (20). Differentially-expressed genes were identified using the Cufflinks tools (Cuffmerge and Cuffdiff). cummeRbund (v 2.4.1) (20) was used to assess replicate concordance. In the second pipeline, reads were mapped against the human reference genome (Ensembl GRCh37) using the aligner STAR (v 2.4.2a), and gene level counts of uniquely mapped reads were obtained using htseq-count (v 0.6.1) (14). Differential expression analysis was performed using DESeq2 (21) for each pairwise condition using a p-adj threshold of 0.05. The FPKM-based method and the counts-based method generated concordant results. Analyses using the FPKM-based method have been represented in results.

Human melanocyte and melanoma transcriptome analysis

Three hundred and eighty-five human RNA-seq samples were downloaded from the Cancer Genomics Hub (CGHub) (https://cghub.ucsc.edu) using GeneTorrent (v 3.8.5a) (22). The RNAseq TCGA dataset is comprised of three sample types: 302 metastatic

melanoma samples, 82 primary melanomas, and 1 solid tissue normal (23). For the normal melanocyte datasets, two RNAseq samples were downloaded from the Short Read Archive (SRA) (https://www.ncbi.nlm.nih.gov/sra/; accession codes: SRR522118, SRR522119)(24) and two from the ENCODE project (https://www.encodeproject.org/; experiment: ENCSR000CUQ) (25). The datasets downloaded from TCGA, SRA and ENCODE were aligned to the human reference genome (Ensembl GRCh37) and analyzed using the FPKM-based method described above.

Supplemental References

1. Bruneau, S., and Rosa, F.M. 1997. Dynamo, a new zebrafish DVR member of the TGF-beta superfamily is expressed in the posterior neural tube and is up-regulated by Sonic hedgehog. *Mech Dev* 61:199-212.
2. Langmead, B., Trapnell, C., Pop, M., and Salzberg, S.L. 2009. Ultrafast and memory-efficient alignment of short DNA sequences to the human genome. *Genome Biol* 10:R25.
3. Heinz, S., Benner, C., Spann, N., Bertolino, E., Lin, Y.C., Laslo, P., Cheng, J.X., Murre, C., Singh, H., and Glass, C.K. 2010. Simple combinations of lineage-determining transcription factors prime cis-regulatory elements required for macrophage and B cell identities. *Mol Cell* 38:576-589.
4. Feng, J., Liu, T., Qin, B., Zhang, Y., and Liu, X.S. 2012. Identifying ChIP-seq enrichment using MACS. *Nat Protoc* 7:1728-1740.
5. Zhu, L.J., Gazin, C., Lawson, N.D., Pages, H., Lin, S.M., Lapointe, D.S., and Green, M.R. 2010. ChIPpeakAnno: a Bioconductor package to annotate ChIP-seq and ChIP-chip data. *BMC Bioinformatics* 11:237.
6. Krzywinski, M., Schein, J., Birol, I., Connors, J., Gascoyne, R., Horsman, D., Jones, S.J., and Marra, M.A. 2009. Circos: an information aesthetic for comparative genomics. *Genome Res* 19:1639-1645.
7. Beroukhim, R., Mermel, C.H., Porter, D., Wei, G., Raychaudhuri, S., Donovan, J., Barretina, J., Boehm, J.S., Dobson, J., Urashima, M., et al. 2010. The landscape of somatic copy-number alteration across human cancers. *Nature* 463:899-905.
8. Lin, W.M., Baker, A.C., Beroukhim, R., Winckler, W., Feng, W., Marmion, J.M., Laine, E., Greulich, H., Tseng, H., Gates, C., et al. 2008. Modeling genomic

diversity and tumor dependency in malignant melanoma. *Cancer Res* 68:664-673.

9. Howe, K., Clark, M.D., Torroja, C.F., Torrance, J., Berthelot, C., Muffato, M., Collins, J.E., Humphray, S., McLaren, K., Matthews, L., et al. 2013. The zebrafish reference genome sequence and its relationship to the human genome. *Nature* 496:498-503.
10. Collins, J.E., White, S., Searle, S.M., and Stemple, D.L. 2012. Incorporating RNA-seq data into the zebrafish Ensembl genebuild. *Genome Res* 22:2067-2078.
11. Altschul, S.F., Gish, W., Miller, W., Myers, E.W., and Lipman, D.J. 1990. Basic local alignment search tool. *J Mol Biol* 215:403-410.
12. S, A. 2010. FastQC: a quality control tool for high throughput sequence data.
13. Dobin, A., Davis, C.A., Schlesinger, F., Drenkow, J., Zaleski, C., Jha, S., Batut, P., Chaisson, M., and Gingeras, T.R. 2013. STAR: ultrafast universal RNA-seq aligner. *Bioinformatics* 29:15-21.
14. Anders, S., Pyl, P.T., and Huber, W. 2015. HTSeq--a Python framework to work with high-throughput sequencing data. *Bioinformatics* 31:166-169.
15. Ritchie, M.E., Phipson, B., Wu, D., Hu, Y., Law, C.W., Shi, W., and Smyth, G.K. 2015. limma powers differential expression analyses for RNA-sequencing and microarray studies. *Nucleic Acids Res* 43:e47.
16. Langmead, B., and Salzberg, S.L. 2012. Fast gapped-read alignment with Bowtie 2. *Nat Methods* 9:357-359.
17. Kim, D., Pertea, G., Trapnell, C., Pimentel, H., Kelley, R., and Salzberg, S.L. 2013. TopHat2: accurate alignment of transcriptomes in the presence of insertions, deletions and gene fusions. *Genome Biol* 14:R36.

18. Li, H., Handsaker, B., Wysoker, A., Fennell, T., Ruan, J., Homer, N., Marth, G., Abecasis, G., and Durbin, R. 2009. The Sequence Alignment/Map format and SAMtools. *Bioinformatics* 25:2078-2079.

19. Thorvaldsdottir, H., Robinson, J.T., and Mesirov, J.P. 2013. Integrative Genomics Viewer (IGV): high-performance genomics data visualization and exploration. *Brief Bioinform* 14:178-192.

20. Trapnell, C., Roberts, A., Goff, L., Pertea, G., Kim, D., Kelley, D.R., Pimentel, H., Salzberg, S.L., Rinn, J.L., and Pachter, L. 2012. Differential gene and transcript expression analysis of RNA-seq experiments with TopHat and Cufflinks. *Nat Protoc* 7:562-578.

21. Love, M.I., Huber, W., and Anders, S. 2014. Moderated estimation of fold change and dispersion for RNA-seq data with DESeq2. *Genome Biol* 15:550.

22. Wilks, C., Cline, M.S., Weiler, E., Diehkans, M., Craft, B., Martin, C., Murphy, D., Pierce, H., Black, J., Nelson, D., et al. 2014. The Cancer Genomics Hub (CGHub): overcoming cancer through the power of torrential data. *Database (Oxford)* 2014.

23. 2015. Genomic Classification of Cutaneous Melanoma. *Cell* 161:1681-1696.

24. Barrett, T., Wilhite, S.E., Ledoux, P., Evangelista, C., Kim, I.F., Tomashevsky, M., Marshall, K.A., Phillippy, K.H., Sherman, P.M., Holko, M., et al. 2013. NCBI GEO: archive for functional genomics data sets--update. *Nucleic Acids Res* 41:D991-995.

25. 2012. An integrated encyclopedia of DNA elements in the human genome. *Nature* 489:57-74.

Uncut blots

Full unedited gel for Fig. 2C

GDF6 and GAPDH in different melanoma cell lines

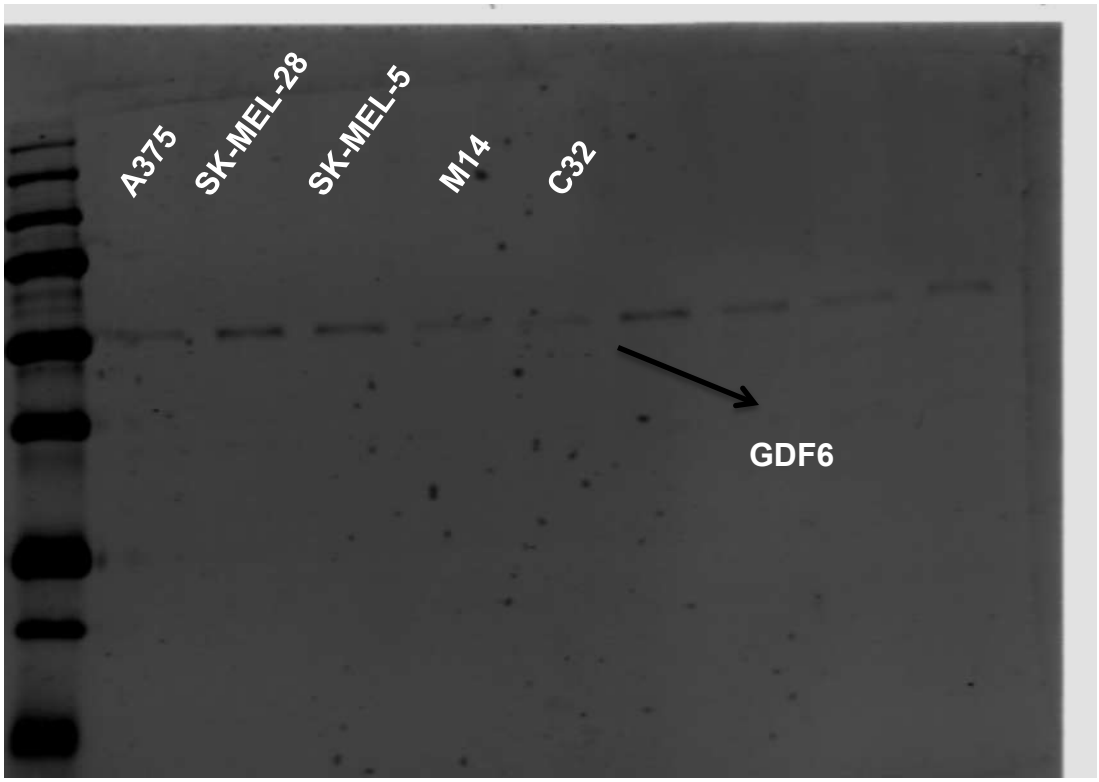

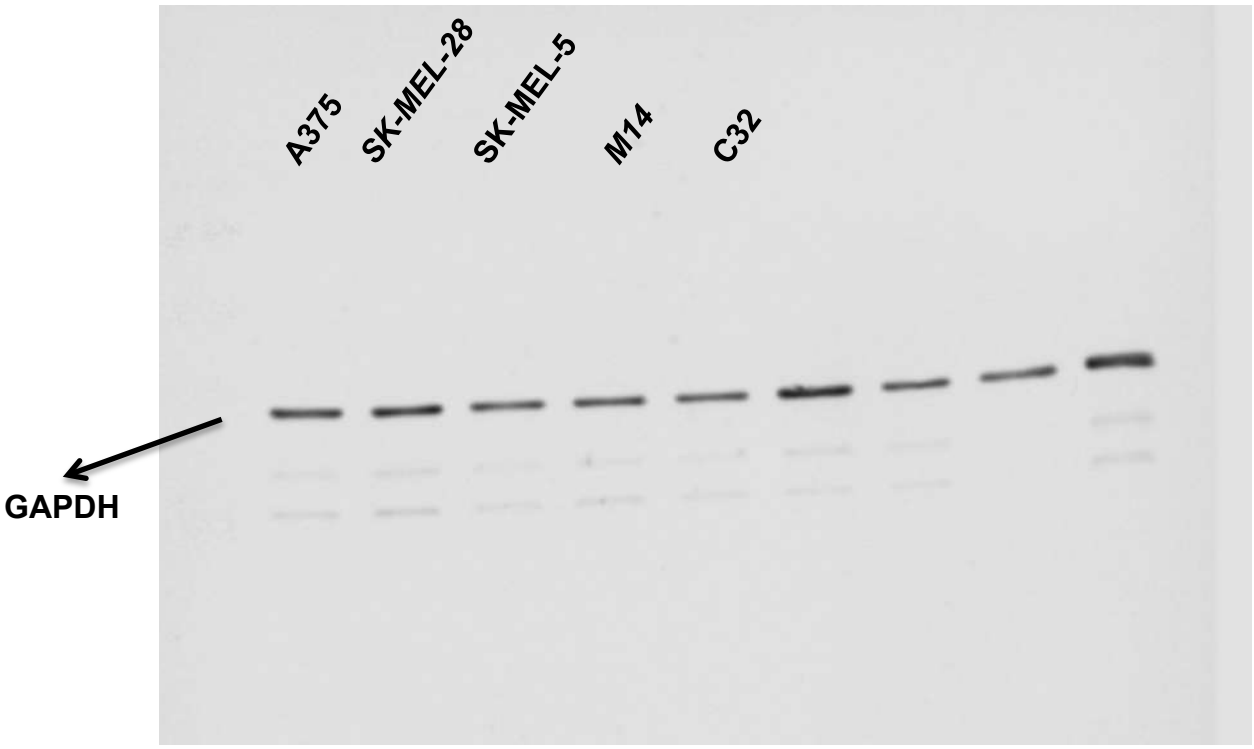

Full unedited gel for Fig. 2D, Fig. S7F

GDF6 and SMAD1DVD overexpression in A375 cells- Flag-SMAD1DVD and GDF6 expression

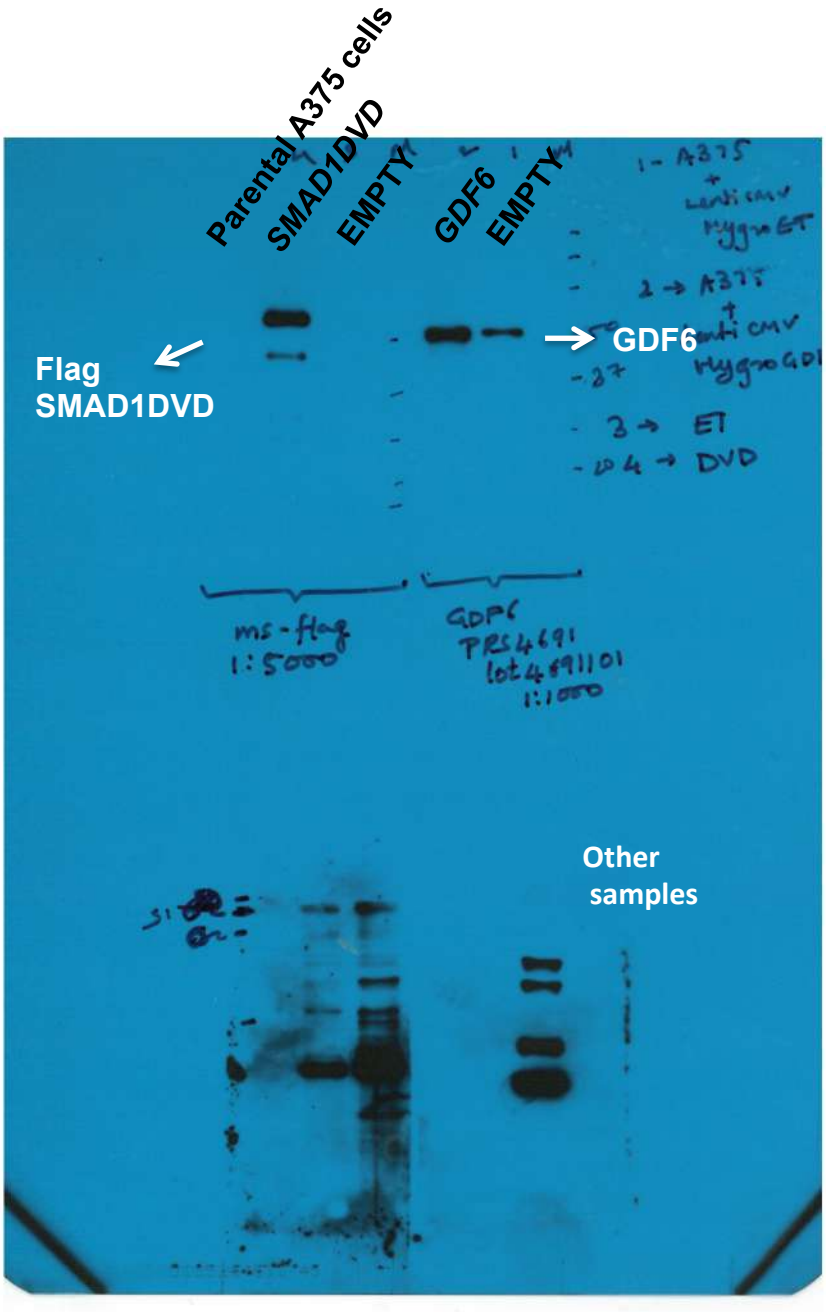

Full unedited gel for Fig. 2D, Fig. S6F

GDF6 and SMAD1DVD overexpression in A375 cells- GAPDH expression

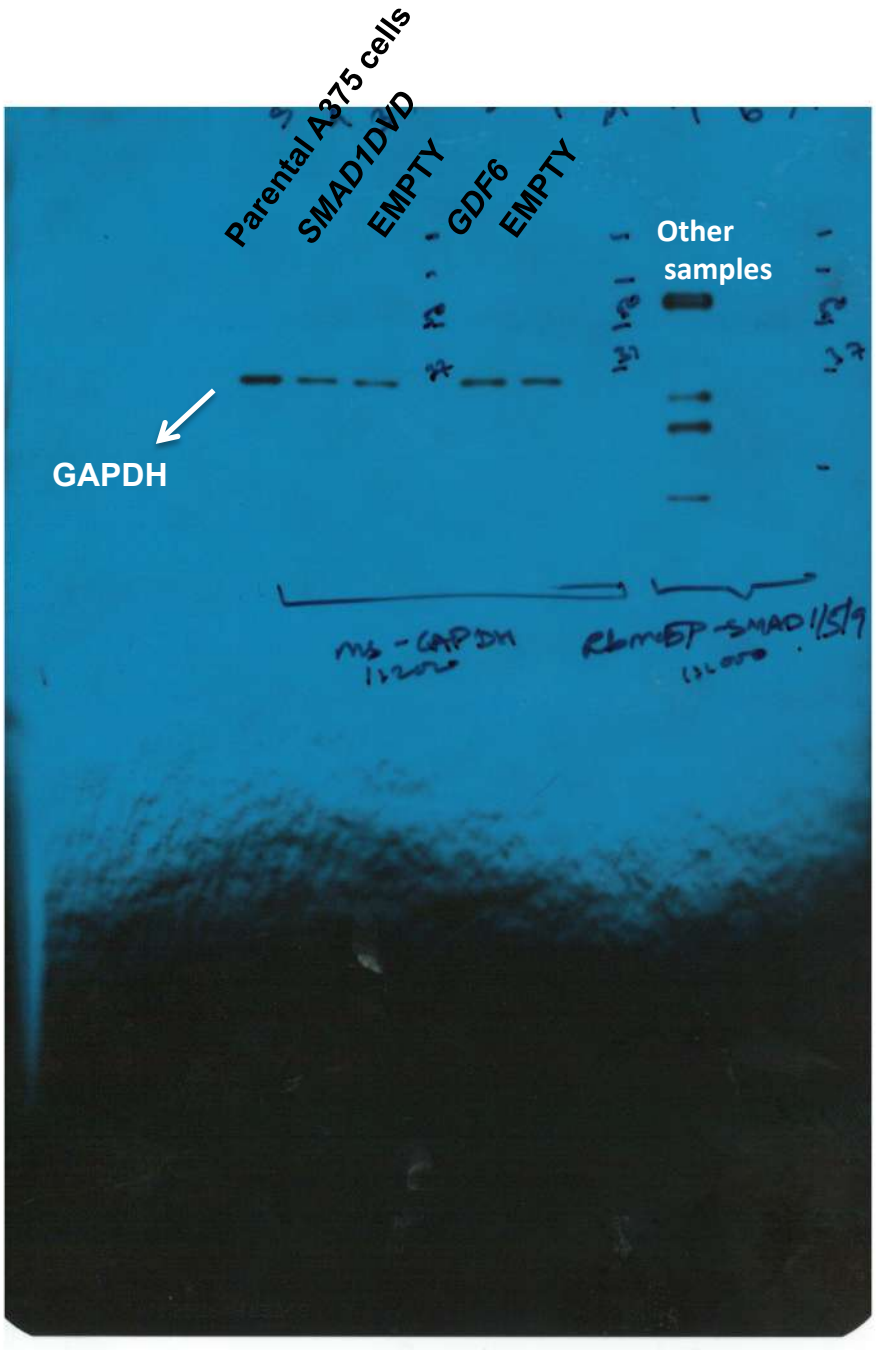

Full unedited gel for Fig. 2D, Fig. S5A

GDf6 overexpression in melanoma cell lines- GDF6 and GAPDH expression

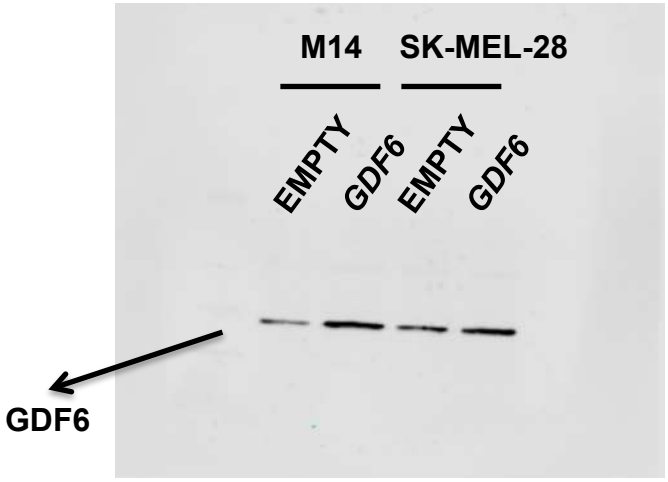

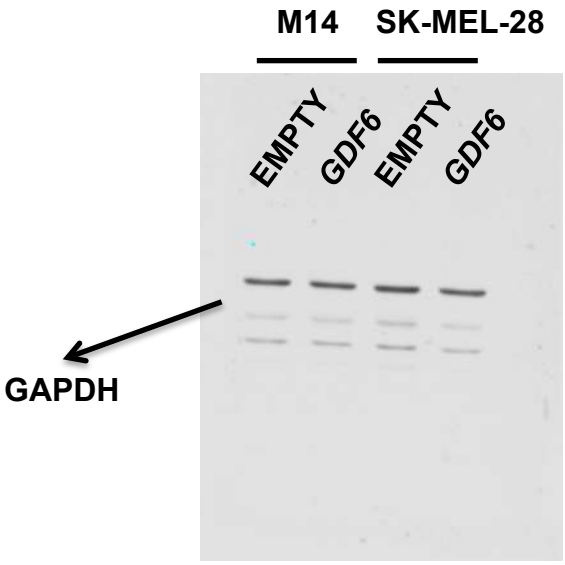

Full unedited gel for Fig. 2F and 3D

1) A375 cells with GDF6 knockdown- GDF6 expression
2) A375 cells with GDF6 knockdown- Total SMAD1/5/8 expression

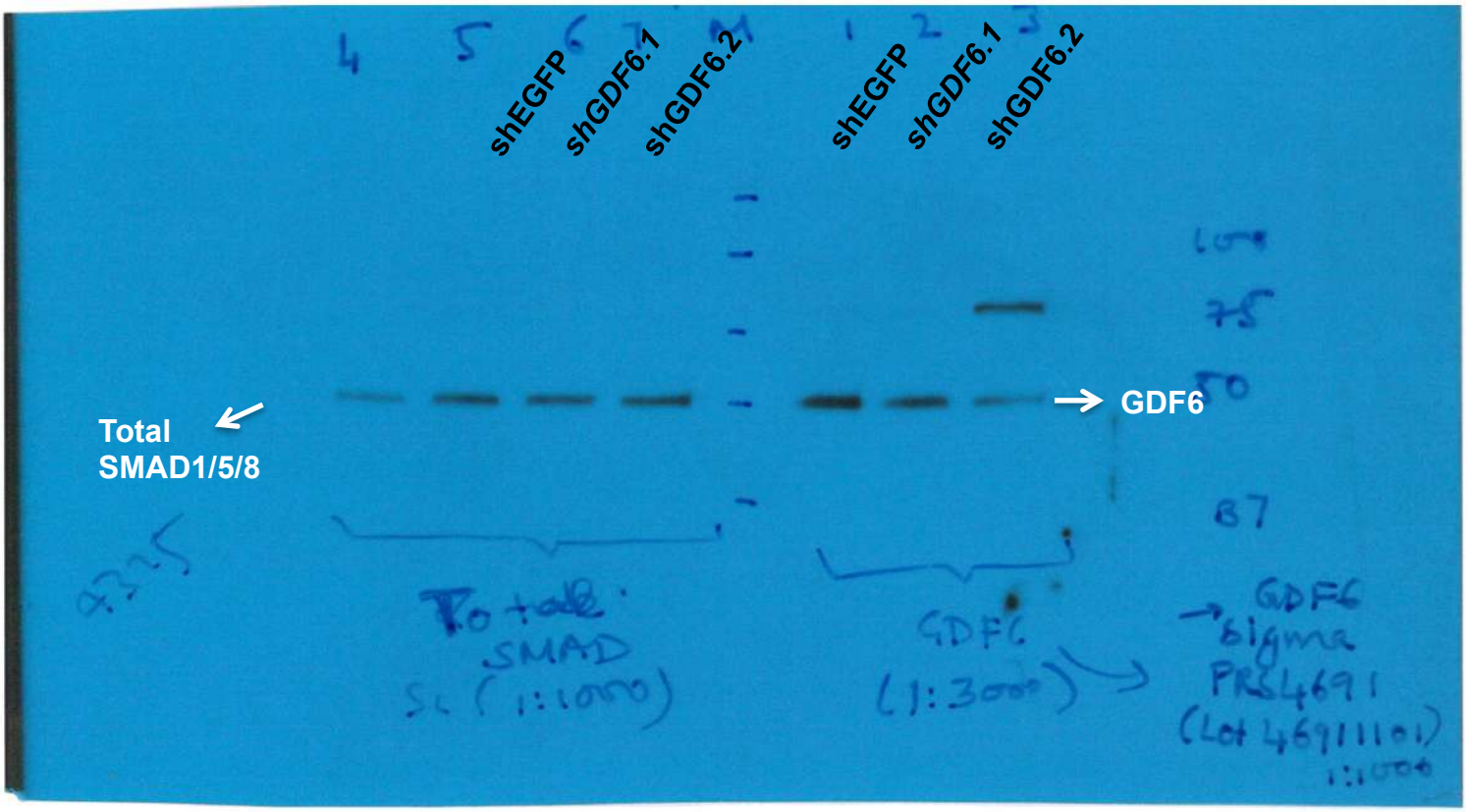

Full unedited gel for Fig. 2F and 3D

1) A375 cells with GDF6 knockdown- GAPDH expression

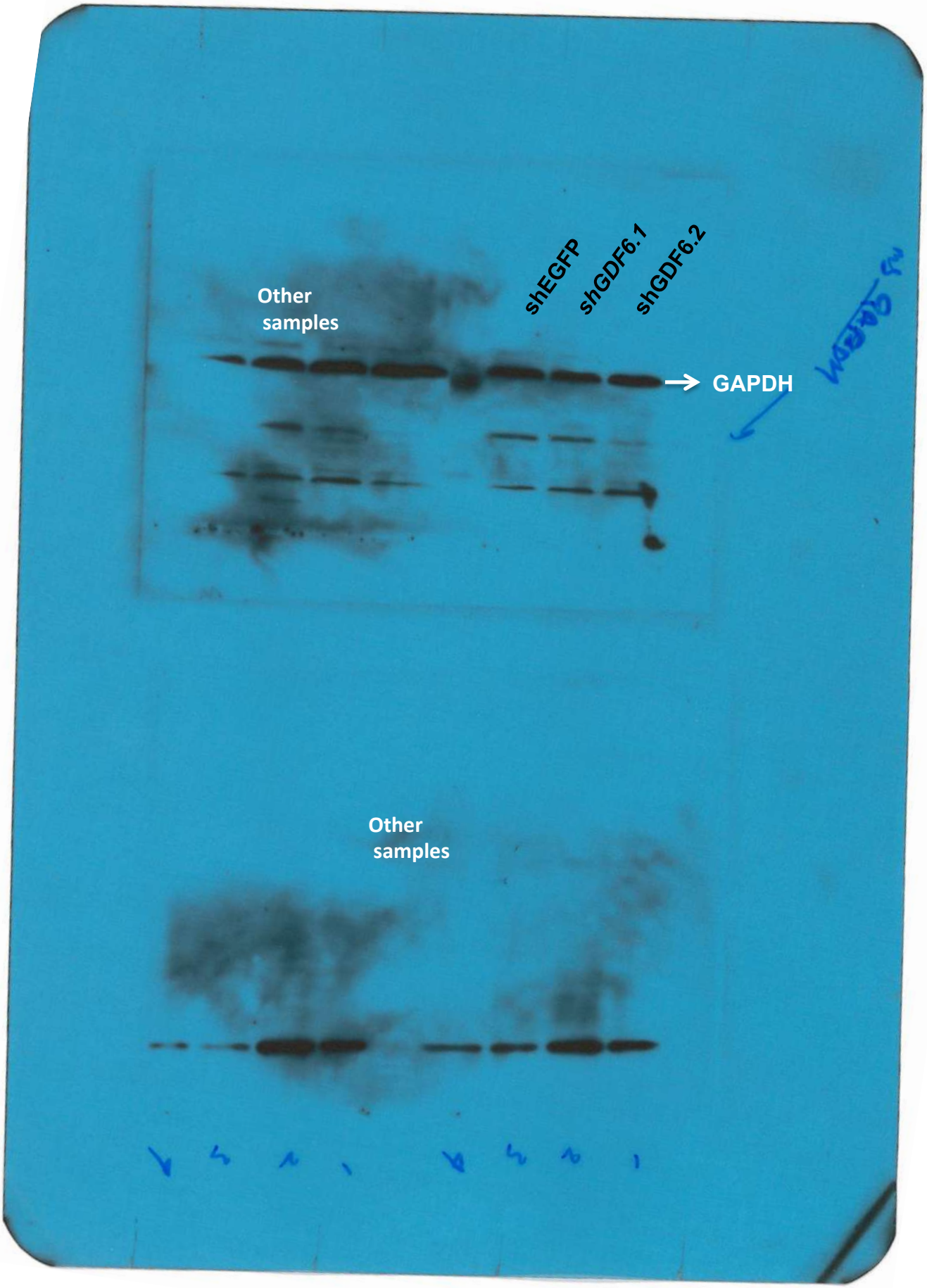

Full unedited gel for Fig. 3D

1) A375 cells with GDF6 knockdown- phosphoSMAD1/5/8 expression

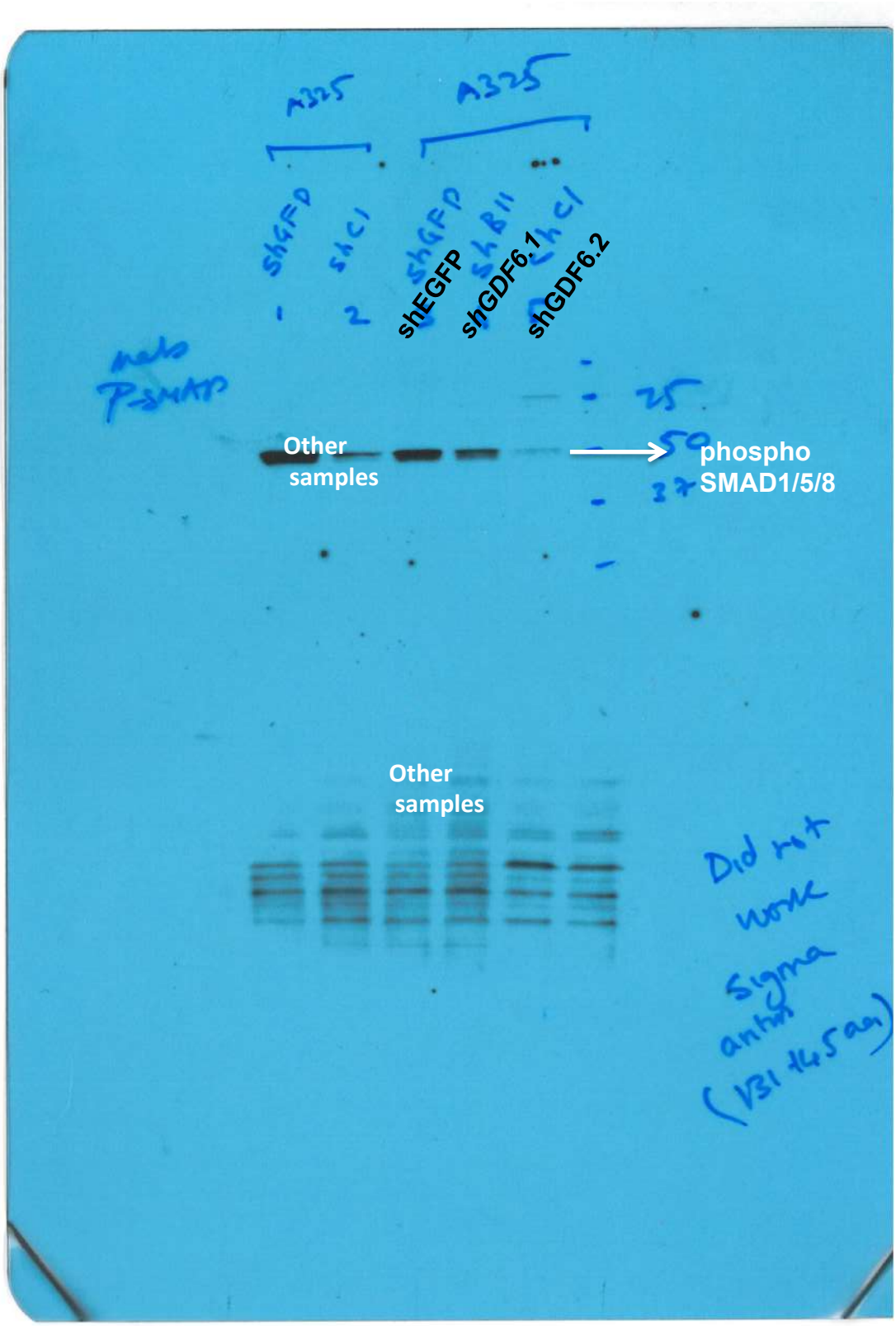

Full unedited gel for Fig. 2F and S5E

GDF6 and GAPDH expression in different melanoma cell lines upon GDF6 knockdown

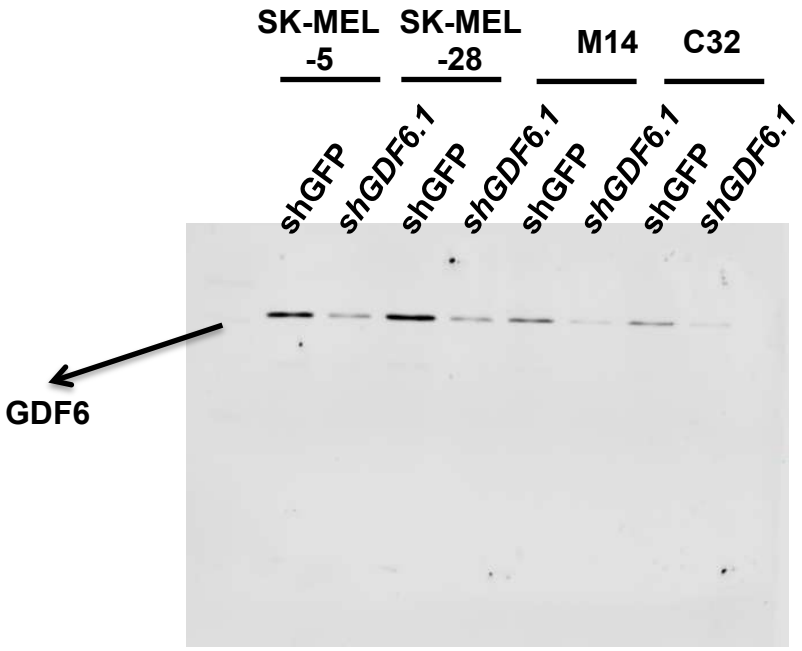

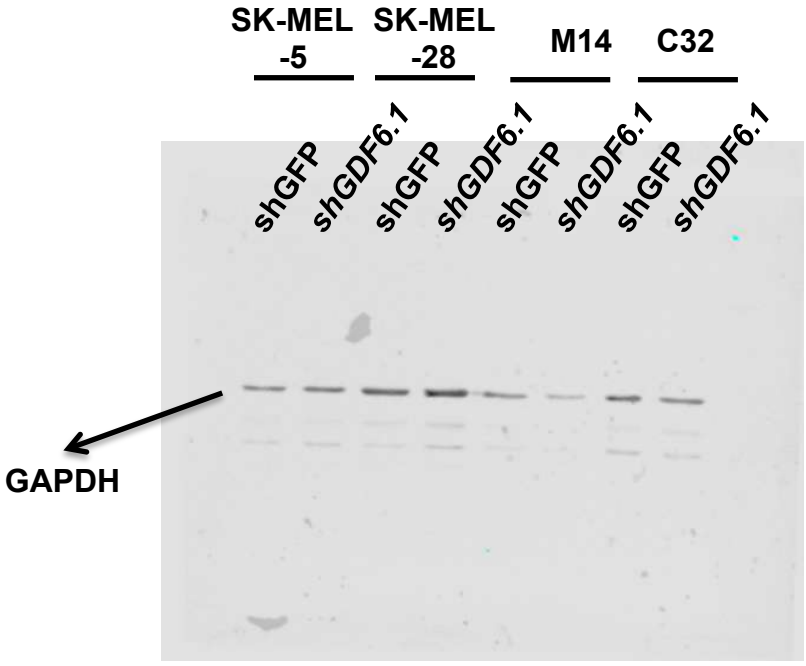

Full unedited gel for Fig. S5H

GDF6 overexpression in A375 cells- phsphoSMAD1/5/8 and GAPDH expression

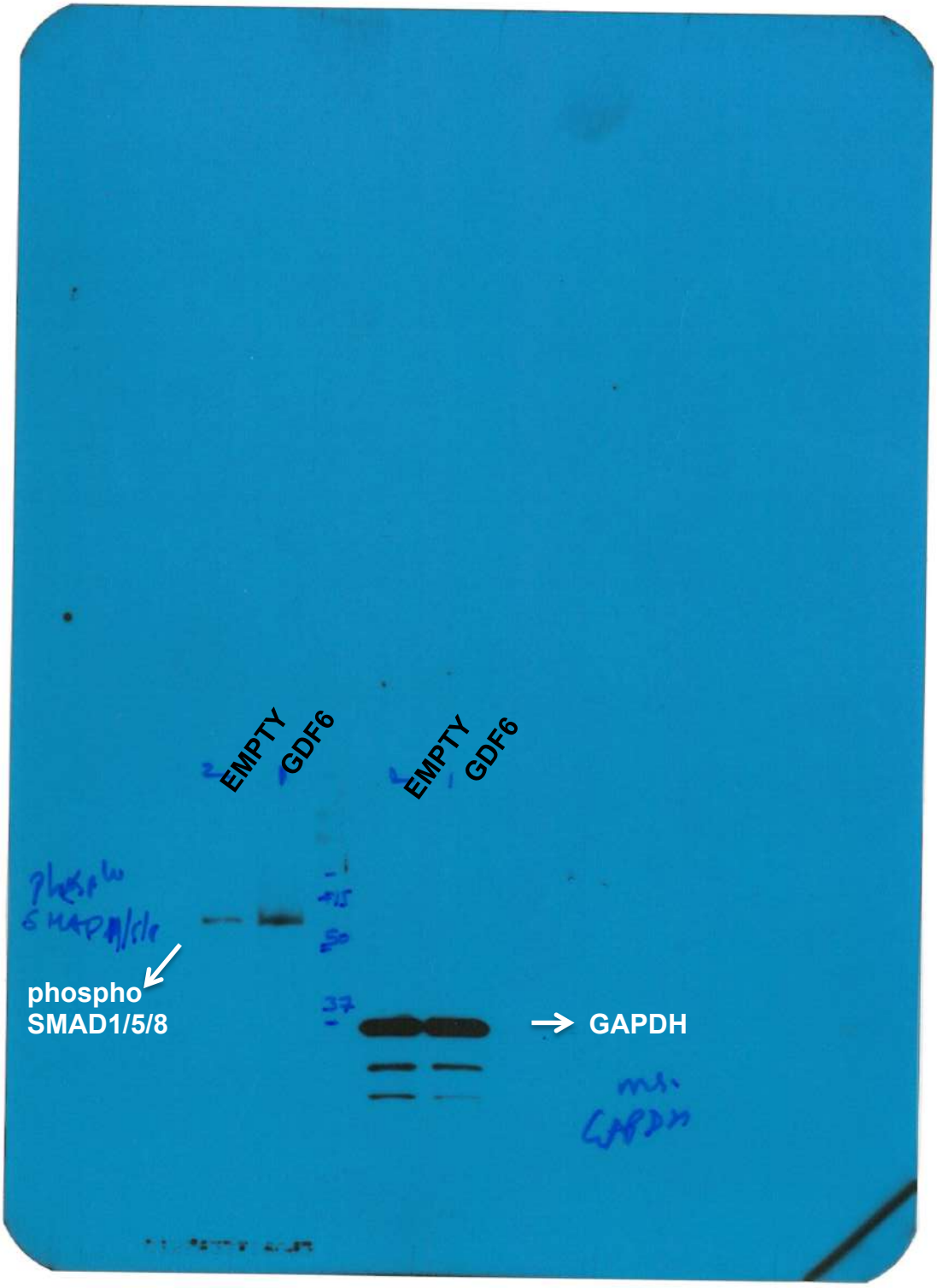

Full unedited gel for Fig. S5H

GDF6 overexpression in A375 cells- Total SMAD1/5/8 expression

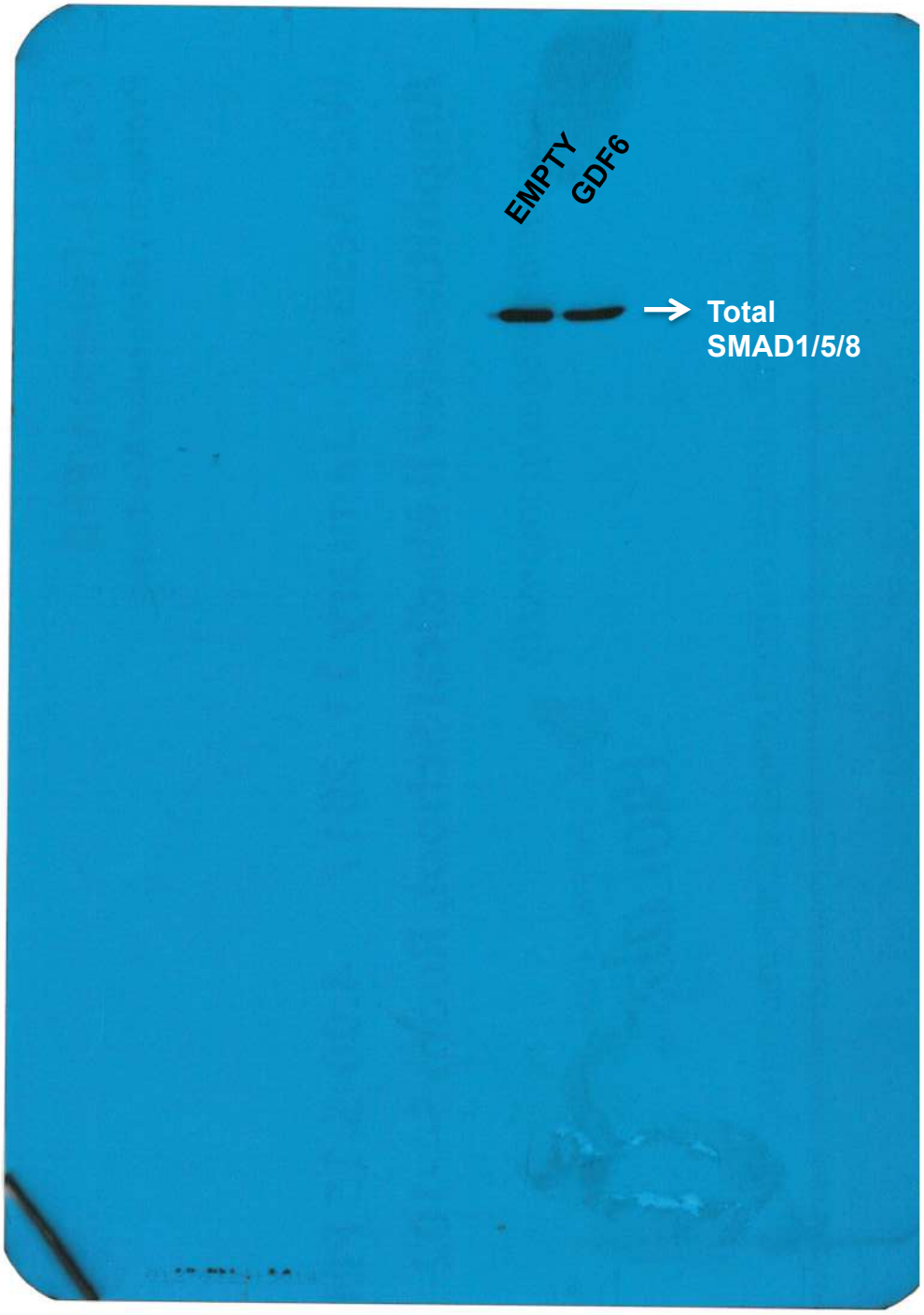

Full unedited gel for Fig. S5H

1) Melanoma cell lines with GDF6 overexpression- phosphoSMAD1/5/8 and total SMAD1/5/8 expression

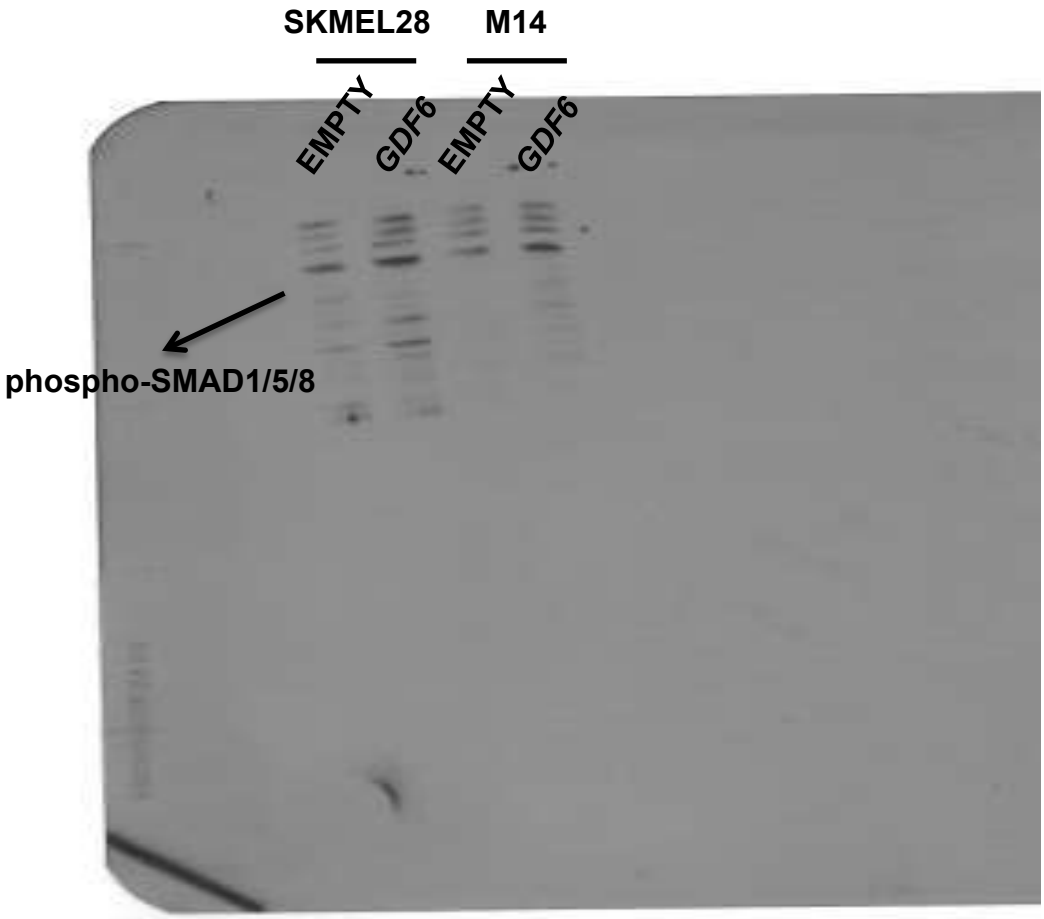

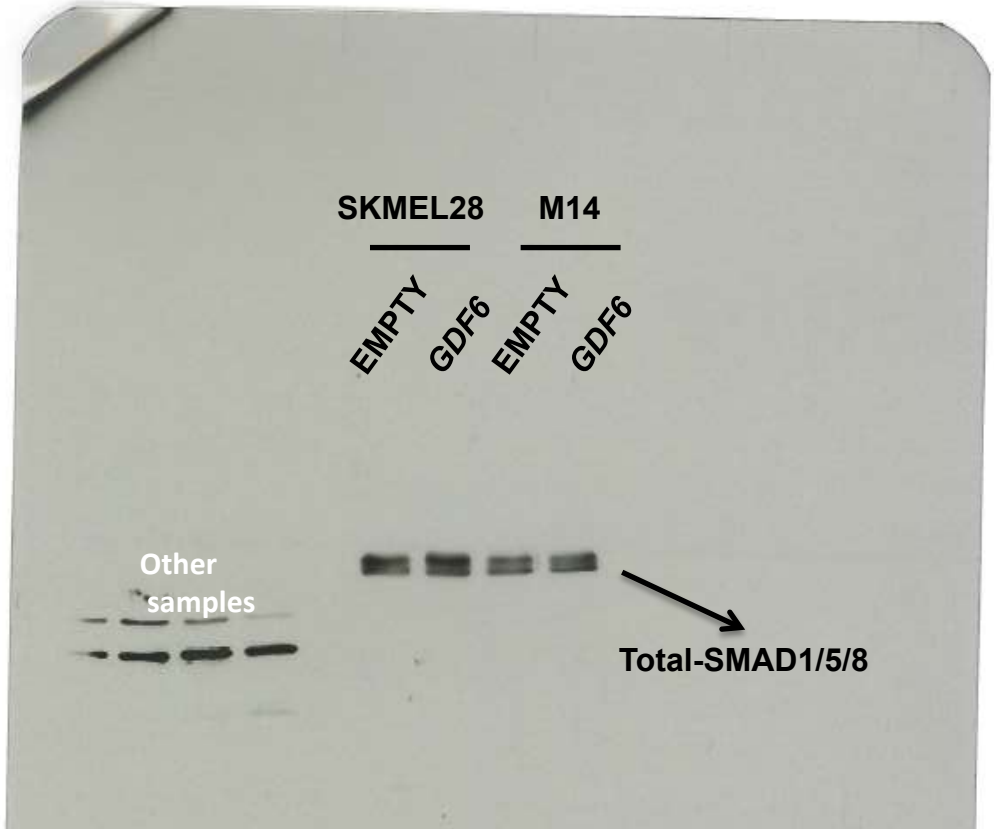

Full unedited gel for Fig. S7A

A375 cells with SMAD1 knockdown- Total SMAD1 and GAPDH expression

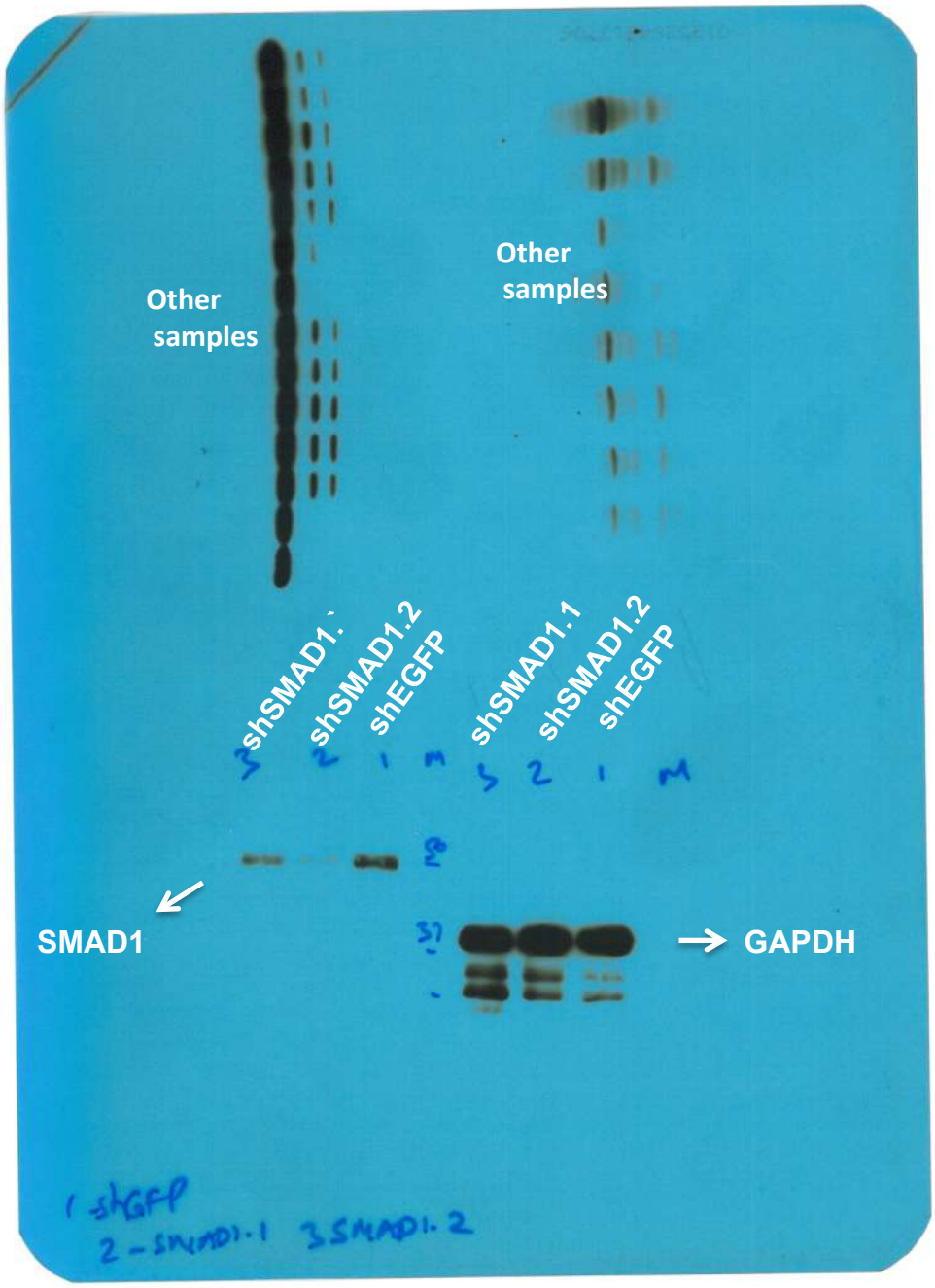

Full unedited gel for Fig. S7D

A375 cells with DMH1 treatment- phsophoSMAD1/5/8

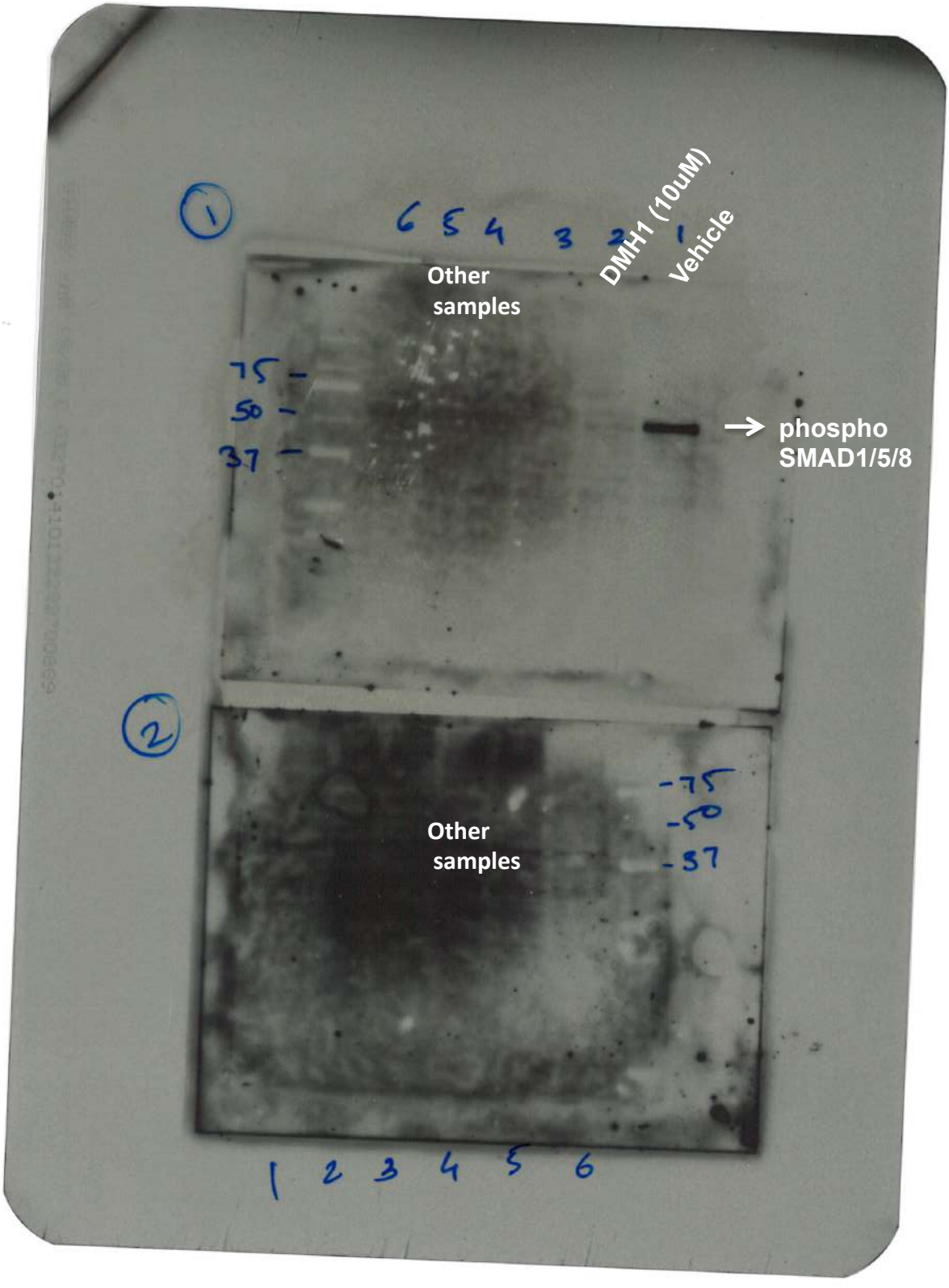

Full unedited gel for Fig. S7D

A375 cells with DMH1 treatment- Total SMAD1/5/8 levels

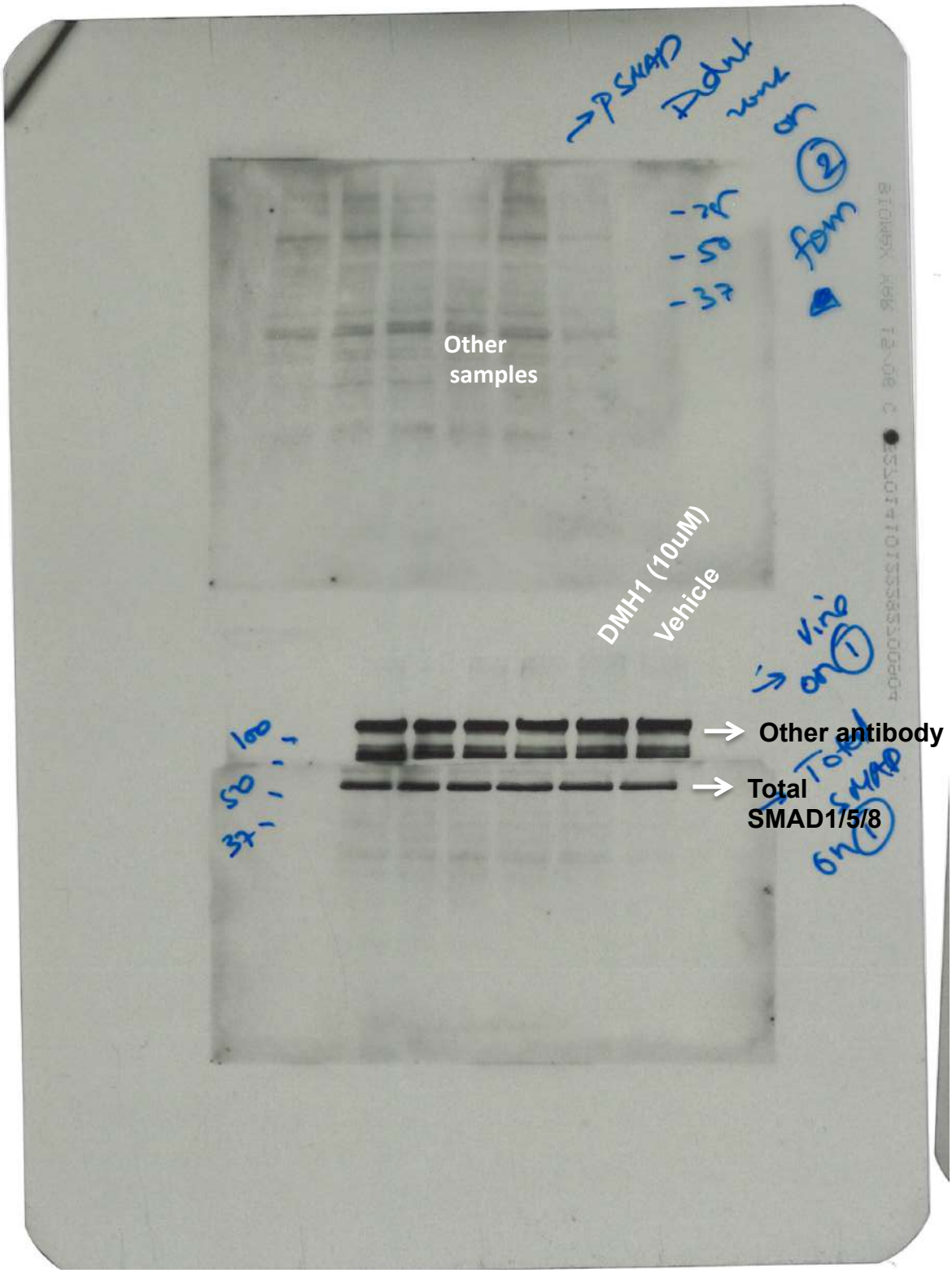

Full unedited gel for Fig. 6E

A375 cells with SMAD1DVD expression upon GDF6 knockdown- SOX9 expression

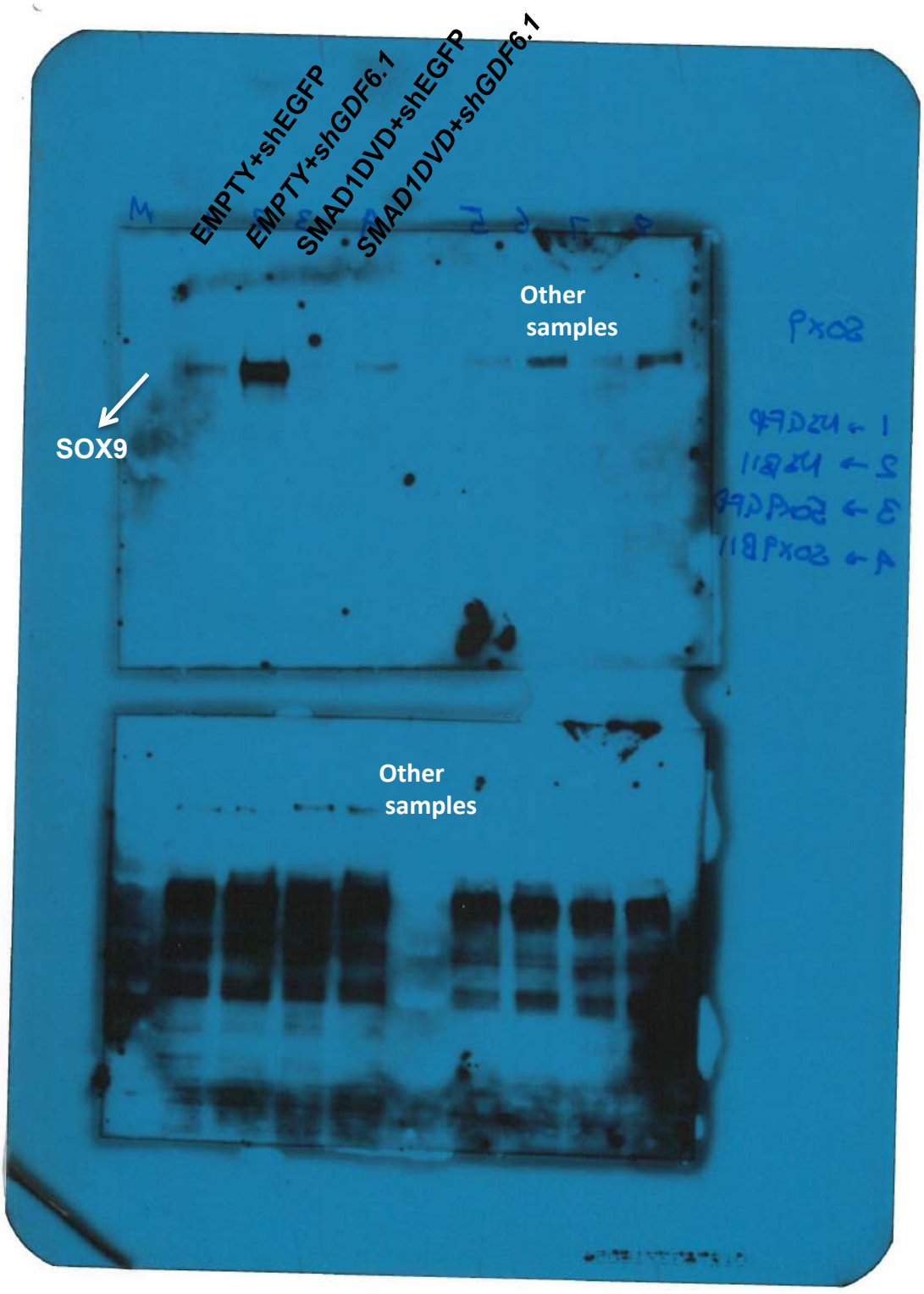

Full unedited gel for Fig. S11D

A375 cells with GDF6/SOX9 knockdown- SOX9 expression

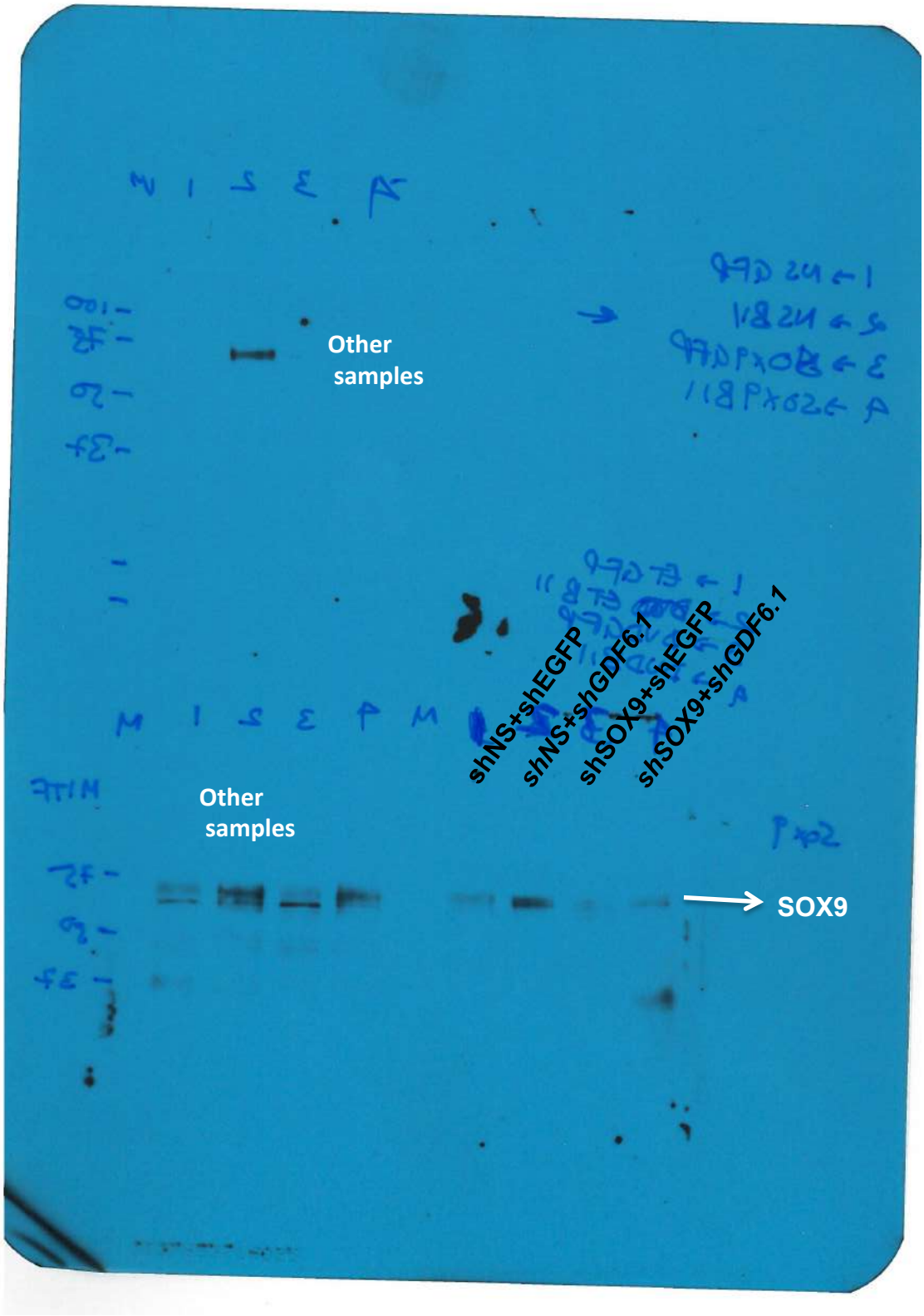

Full unedited gel for Fig. 6E and Fig. S11D

1) A375 cells with SMAD1DVD expression upon GDF6 knockdown- GAPDH expression

2) A375 cells with GDF6/SX9 knockdown- GAPDH expression